Magnon spin photogalvanic effect induced by Aharonov-Casher phase

YuanDong Wang [1,2] Zhen-Gang Zhu [1,2,3,*] and Gang Su [2,3,4,†]

[1]*School of Electronic, Electrical and Communication Engineering, University of Chinese Academy of Sciences, Beijing 100049, China*

[2]*School of Physical Sciences, University of Chinese Academy of Sciences, Beijing 100049, China*

[3]*CAS Center for Excellence in Topological Quantum Computation, University of Chinese Academy of Sciences, Beijing 100049, China*

[4]*Kavli Institute for Theoretical Sciences, University of Chinese Academy of Sciences, Beijing 100190, China*

(Received 12 April 2024; revised 25 July 2024; accepted 30 July 2024; published 22 August 2024)

Magnons are electrically neutral bosonic quasiparticles emerging as collective spin excitations of magnetically ordered materials, and they play a central role in next-generation spintronics due to its obviating Joule heating. A difficult obstacle for quantum magnonics is that the magnons do not couple to the external electric field directly so that a direct electric manipulation via bias or gate voltage as in conventional charge-based devices seems not to be applicable. In this work, we propose a mechanism in which magnons can be excited and controlled by an electric field of light directly. Since the electric field of light can be tuned in a wide and easy way, the proposal should be of great interest in realistic applications. We call it the magnon spin photogalvanic effect (SPGE), which comes from five contributions: Drude, Berry curvature dipole (BCD), injection, shift, and rectification, with distinct geometric origins. We further show that the responses to linearly polarized or circularly polarized light are determined by a band-resolved quantum metric or Berry curvature, both of which, when combined, comprise a quantum geometric tensor. The proposed magnon SPGE can be measured by a characterized topological phase transition. We also discuss a breathing kagome-lattice model of ferromagnets, and we suggest possible candidate materials to implement it.

DOI: 10.1103/PhysRevB.110.054434

I. INTRODUCTION

Spin transport plays a central role in the field of spintronics [1,2]. Currently there is significant interest in exploring the magnons in magnetic materials. The magnons, which are collective spin excitations of magnetically ordered materials, are electrically neutral bosonic quasiparticles. The transport of magnons obviates Joule heating at a fundamental level, and thus magnons are regarded as a candidate with which to pursue next-generation spintronics [3,4]. For this purpose, a deeper understanding of the properties of magnons and their precise manipulation is urgently called for. However, due to the electrical neutrality of magnons, their coupling to an external electric field has been considered less frequently. Therefore, much of the progress has been made in studying the thermal control of magnons [5–12]. However, thermal control is not easy to maintain accurately, and sometimes it is even cumbersome.

One of the most promising approaches is to use the optical method to control the magnons. Since magnons possess spin degrees of freedom, it has been proposed that the dc magnon spin photocurrent (MSPC) can be generated in antiferromagnets by the Zeeman coupling of magnon spin and the magnetic field component of light, where the angular momentum transfer between magnons and photons is invoked by applying a circularly polarized (CP) light [13]. Using the magnetic field component, the generation of the MSPC via linearly polarized (LP) light has been proposed recently [14,15]. A desired goal is to achieve an enhanced MSPC by using the electric field component of the light. For example, the MSPC driven by CP light was proposed via a two-magnon Raman process with coupling to the electric field [16]. It is a direct spin angular momentum transfer process in which right-handed photons turn into left-handed photons by imparting spin angular momentum and creating a magnon pair carrying a net spin current. Therefore, the current is proportional to the chirality of the incident light, and it vanishes if the light is linearly polarized. The magnetoelectric coupling generally exists in multiferroic materials, for which the magnon can be generated and controlled by an electric field [17–19]. Recently, the MSPC has been predicted in collinear antiferromagnets via the coupling between electric field and polarization with a broken inversion symmetry [20]. Nevertheless, the spin photocurrent induced by the interaction between the electric field and the magnons has not been fully understood, and it is unclear how it is affected by the quantum geometry of magnon bands [21].

In this paper, we develop a general formalism for the MSPC mediated via the Aharonov-Casher (AC) effect of magnons induced by an electric field. It can be understood that magnons moving in an electric field acquire a geometric phase through the AC effect during the processing as [22–24]

$$\theta_{ij} = \frac{g\mu_B}{\hbar c^2}\int_{r_i}^{r_j}[\boldsymbol{E}(t)\times\hat{\boldsymbol{e}}_z]\cdot d\boldsymbol{r}, \tag{1}$$

where $\boldsymbol{E}(t)$ is the electric field of light. In Eq. (1) we assume that the magnetization is along the z-direction and then the magnetic moment of magnon points in the $-z$-direction with

*Contact author: zgzhu@ucas.ac.cn

†Contact author: gsu@ucas.ac.cn

$\boldsymbol{\mu} = -g\mu_B\hat{\boldsymbol{e}}_z$, where g is the Landé factor and μ_B is the Bohr magneton. This phase (θ_{ij}) will enter into the coupling between spins or the hopping integral of electron operators (see Appendixes A and B). The Hamiltonian is thus modified in a form in which the effect of the electric field of light will serve as a driving force. Because this electric field couples to the local magnetization, magnons (variations of magnetization) will consequently be excited.

II. THEORETICAL FRAMEWORK

A. Light-magnon coupling and density matrix equations of motion

For a general two-body spin interaction Hamiltonian in the absence of an external field,

$$H_0 = \frac{1}{2}\sum_{i,j}^{L}\sum_{n,m}^{N}\sum_{\alpha\beta} S_{i,n}^{\alpha} H_{nm}^{\alpha\beta}(i-j) S_{j,m}^{\beta}, \tag{2}$$

where $\boldsymbol{S}_{i,n}$ is a spin operator at the nth sublattice (with total number N) of the ith magnetic unit cell (with total number L), with $H_{nm}^{\alpha\beta}(i-j)$ the magnetic exchange interaction. The classical ground state is identified by treating the quantum-mechanical spin operators as classical vectors and minimizing the classical ground-state energy. By setting the global (reference) coordinates $(\hat{\boldsymbol{x}}, \hat{\boldsymbol{y}}, \hat{\boldsymbol{z}})$, the local coordinates (spherical coordinates) of each spin are related to the global coordinates via $\boldsymbol{S}_{i,n} = R_n(\theta_i, \phi_i)\boldsymbol{S}_0$. The magnons are the usual low-energy excitations in ordered magnets, which are considered via the Holstein-Primakoff transformation in local coordinates [25],

$$\begin{aligned} &S_{i,n}^{\theta} = \sqrt{\frac{S}{2}}(a_{i,n} + a_{i,n}^{\dagger}), \quad S_{i,n}^{\phi} = -i\sqrt{\frac{S}{2}}(a_{i,n} - a_{i,n}^{\dagger}), \\ &S_{i,n}^{r} = S - a_{i,n}^{\dagger}a_{i,n}, \end{aligned} \tag{3}$$

and we obtain

$$\boldsymbol{S}_{i,n}^{\alpha} = \sqrt{\frac{S}{2}}\hat{\boldsymbol{u}}_n a_{i,n} + \sqrt{\frac{S}{2}}\hat{\boldsymbol{u}}_n^{*} a_{i,n}^{\dagger} + \hat{\boldsymbol{z}}_n(S - a_{i,n}^{\dagger}a_{i,n}), \tag{4}$$

where $\alpha = x, y, z$, and the coefficients $\hat{\boldsymbol{u}}_n$ and $\hat{\boldsymbol{z}}_n$ are related to the relative rotation between the global and local coordinates. Using Eq. (4) and the transformation into the momentum space, the magnon Hamiltonian is written as $H = \frac{1}{2}\sum_{\boldsymbol{k}} \Psi_{\boldsymbol{k}}^{\dagger}\mathcal{H}(\boldsymbol{k})\Psi_{\boldsymbol{k}}$, with the kernel $\mathcal{H}(\boldsymbol{k})$ being a $2N \times 2N$ bosonic Bogoliubov–de Gennes (BdG) Hamiltonian with the vector boson operator, where $\Psi_{\boldsymbol{k}}^{\dagger} = (a_{\boldsymbol{k},1}^{\dagger}, \ldots, a_{\boldsymbol{k},N}^{\dagger}, a_{-\boldsymbol{k},1}, \ldots, a_{-\boldsymbol{k},N})$ [for details on $\mathcal{H}(\boldsymbol{k})$, see Appendix A].

In general, the bosonic Hamiltonian $\mathcal{H}(\boldsymbol{k})$ does not conserve the particle number, e.g., the ferromagnets with elliptical magnons (where an anisotropy deforms the formerly circular precession) or in nonferromagnets. In addition, the Hamiltonian is diagonalized with the Bogoliubov transformation

$$U_{\boldsymbol{k}}^{\dagger}\mathcal{H}_{\boldsymbol{k}}U_{\boldsymbol{k}} = \mathcal{E}_{\boldsymbol{k}}, \tag{5}$$

which satisfies $U_{\boldsymbol{k}}\Sigma_z U_{\boldsymbol{k}}^{\dagger} = \Sigma_z$, where the diagonal matrix $\Sigma_z = \mathrm{diag}(1, 1, \ldots, -1, -1, \ldots)$ with N positive 1's and N minus 1's along the diagonal. The vector boson operator transforms as $\Psi_{\boldsymbol{k}} = U_{\boldsymbol{k}}\Phi_{\boldsymbol{k}}$. The mth column vector encoded in the matrix $U_{\boldsymbol{k}}$ stands for the (periodic part of the) Bloch wave function for the mth magnon band [26]. Note that $\Phi_{\boldsymbol{k}}$ does not satisfy the commutation relation of bosons. Instead it satisfies

$$[\Phi_{\boldsymbol{k}}, \Phi_{\boldsymbol{k}'}^{\dagger}] = \Sigma_z\delta_{\boldsymbol{k},\boldsymbol{k}'}. \tag{6}$$

The equilibrium density matrix in band space is given as

$$\rho_{\boldsymbol{k}m}^{(0)}(t) \equiv \langle(\Phi_{\boldsymbol{k}}^{\dagger})_m(t)(\Phi_{\boldsymbol{k}})_m(t)\rangle_0, \tag{7}$$

where the subscript "0" denotes the equilibrium state, and $(\Phi_{\boldsymbol{k}}^{\dagger})_m$ is the mth element of the vector $\Phi_{\boldsymbol{k}}^{\dagger}$. For later convenience, we write $(\Phi_{\boldsymbol{k}}^{\dagger})_m$ as $\Phi_{\boldsymbol{k}m}^{\dagger}$. By using Eq. (6), one obtains

$$\rho_{\boldsymbol{k}m} = \begin{cases} g(\mathcal{E}_{\boldsymbol{k}m}), & [\Phi_{\boldsymbol{k}m}, \Phi_{\boldsymbol{k}m}^{\dagger}] = 1, \\ -g(-\mathcal{E}_{\boldsymbol{k}m}), & [\Phi_{\boldsymbol{k}m}, \Phi_{\boldsymbol{k}m}^{\dagger}] = -1, \end{cases} \tag{8}$$

where $g(\mathcal{E}_{\boldsymbol{k}m})$ is the Bose-Einstein distribution $g(\mathcal{E}_{\boldsymbol{k}m}) = 1/(e^{\beta\mathcal{E}_{\boldsymbol{k}m}} - 1)$, which is abbreviated as g_m in the following. It is convenient to introduce the matrix $\varepsilon_{\boldsymbol{k}}$ [20]:

$$\varepsilon_{\boldsymbol{k}} = \Sigma_z\mathcal{E}_{\boldsymbol{k}} = U_{\boldsymbol{k}}^{-1}\Sigma_z\mathcal{H}_{\boldsymbol{k}}U_{\boldsymbol{k}}, \tag{9}$$

and the density matrix is simplified as $\rho_{\boldsymbol{k}m} = \Sigma_{z,mm}g(\varepsilon_{\boldsymbol{k}m})$. For a general operator, with Bogoliubov's representation, it transforms as

$$\hat{O} = \sum_{\boldsymbol{k}}\Psi_{\boldsymbol{k}}^{\dagger}O_{\boldsymbol{k}}\Psi_{\boldsymbol{k}} = \sum_{\boldsymbol{k}}\Phi_{\boldsymbol{k}}^{\dagger}\Sigma_z\tilde{O}_{\boldsymbol{k}}\Phi_{\boldsymbol{k}}, \tag{10}$$

with the definition $\tilde{O}_{\boldsymbol{k}} = U_{\boldsymbol{k}}^{-1}\Sigma_z O U_{\boldsymbol{k}}$.

There are two ways for the electric field to enter into the Hamiltonian. First, introducing an "electric" vector potential $\boldsymbol{A}^E \equiv \frac{1}{c}\boldsymbol{E}(t) \times \hat{\boldsymbol{e}}_z$ [27–30] (see Appendix B), we have

$$\mathcal{H}(\boldsymbol{k}) = \mathcal{H}_0\left(\boldsymbol{k} + \frac{g\mu_B}{c}\boldsymbol{A}^E\right) \tag{11}$$

via the minimal coupling scheme and making use of the Peierls substitution. Secondly, introducing an effective "electric field" $\tilde{\boldsymbol{E}}(t) = -\partial\boldsymbol{A}^E/\partial t$, the Hamiltonian is modified in the dipole interaction scheme (see Appendix C)

$$\mathcal{H}(t) = \mathcal{H}_0(\boldsymbol{k}) + \frac{g\mu_B}{c}\tilde{\boldsymbol{E}}(t)\cdot\boldsymbol{r}. \tag{12}$$

In Eq. (12), the second term is just the effective dipole interaction.

Recently, it was recognized that the operator $\boldsymbol{r}$ in the crystal lattice is linked to the Berry curvature of Bloch bands of magnons in momentum space. Thus, a covariant derivative operator rather than a usual partial over the momentum to $\boldsymbol{r}$ must be introduced, which is given by [31,32]

$$(\boldsymbol{D}_{\boldsymbol{k}}O_{\boldsymbol{k}})_{mn} = \nabla_{\boldsymbol{k}}O(\boldsymbol{k})_{mn} - i[\boldsymbol{\mathcal{A}}_{\boldsymbol{k}}, O(\boldsymbol{k})]_{mn}, \tag{13}$$

where $\boldsymbol{\mathcal{A}}_{\boldsymbol{k}}$ is the Berry connection whose matrix elements are $\boldsymbol{\mathcal{A}}_{\boldsymbol{k}mn} = i\langle u_{\boldsymbol{k}m}|\nabla_{\boldsymbol{k}}u_{\boldsymbol{k}n}\rangle$, with $|u_{\boldsymbol{k}n}\rangle$ the periodic part of the Bloch functions, and O is an operator. The definition of the covariant derivative operator in Eq. (13) applies to the general magnetic ground state when the magnon Hamiltonian takes the unified transformation $\mathcal{H}(\boldsymbol{k}) \to \mathcal{H}(\boldsymbol{k} - \frac{g\mu_b}{\hbar c}\boldsymbol{A}^E)$ in the presence of an AC phase. The perturbed Hamiltonian is formally the same as the electron Hamiltonian in the presence of an electric field (though the vector potential and the coefficient in front are different).

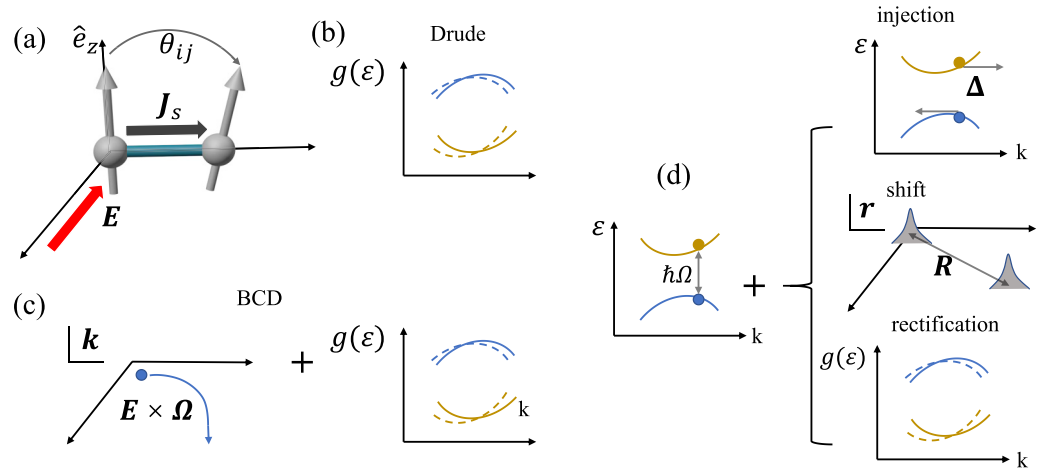

FIG. 1. (a) A schematic of the magnon spin current generated via AC effect with time-dependent electric field. It requires a nonzero electric field along the direction perpendicular to magnetization. (b)–(d) Schematics of five different magnon SPGE currents: (b) the Drude contribution is solely dominated by the nonequilibrium distribution [the dashed (solid) lines represent the distribution with (without) electric field]; (c) the BCD magnon spin current, which is determined by the anomalous velocity and the nonequilibrium distribution; (d) the injection, shift, and rectification spin currents give a combined effect of the dipole transition and group velocity, positional shift, and nonequilibrium distribution.

The effect of the electric field is thus incorporated into the von Neumann equation (see Appendix E) as the optical driving term ($\mathcal{D}_{\rm opt}$ term)

$$(\partial_t + i\varepsilon_{\boldsymbol{k}mn}/\hbar)\rho_{\boldsymbol{k}mn}(t) = \mathcal{D}_{\rm opt}[\rho(t)]_{\boldsymbol{k}mn}, \tag{14}$$

where $\varepsilon_{\boldsymbol{k}mn} = \varepsilon_{\boldsymbol{k}m} - \varepsilon_{\boldsymbol{k}n}$, $\rho_{\boldsymbol{k}mn}(t) \equiv \langle \Phi^\dagger_{\boldsymbol{k}m}\Phi_{\boldsymbol{k}n}\rangle$ is the reduced density matrix in band space given by the average of the product of a creation and a destruction operator in Bloch states, and

$$\mathcal{D}_{\rm opt}[O] = \frac{g\mu_B}{\hbar c^2}\boldsymbol{E}(t)\times\boldsymbol{e}_z\cdot\boldsymbol{D}_{\boldsymbol{k}}[O]. \tag{15}$$

The von Neumann equation can be solved by expanding $\rho = \sum_{n=0}\rho^{(n)}$, where the zero-order density matrix is the Bose-Einstein distribution $\rho^{(0)}_{\boldsymbol{k}mn} = g_{\boldsymbol{k}m}\delta_{mn}$. The recursion equations for the reduced density matrices are obtained as

$$\rho^{(n+1)}_{mn}(\omega) = d_{mn}(\omega)\int\frac{d\omega_1}{2\pi}\omega_1\mathcal{D}_{\rm opt}[\rho^{(n)}(\omega-\omega_1)]_{mn}, \tag{16}$$

with $d_{mn}(\omega) = 1/(\hbar\omega + i0^+ - \varepsilon_{mn})$.

B. Magnon spin current

Due to the conservation of the z component of the total spin, the local magnon spin density $n(\boldsymbol{r}_i) = \hbar\sum_m z_m a^\dagger_{i,m}a_{i,m}$ satisfying the continuity equation $\partial n_{\boldsymbol{q}}/\partial t + i\boldsymbol{q}\cdot\boldsymbol{J}_s = 0$ [$n_{\boldsymbol{q}}$ is a Fourier component of $n(\boldsymbol{r}_i)$] in the long-wavelength limit. The magnon spin current operator is found as (see Appendix D)

$$\hat{\boldsymbol{J}}_s = \hbar\sum_{\boldsymbol{k}}\Phi^\dagger_{\boldsymbol{k}}(\partial_{\boldsymbol{k}}\mathcal{H}_{\boldsymbol{k}} - i[\boldsymbol{\mathcal{A}}_{\boldsymbol{k}},\mathcal{H}_{\boldsymbol{k}}])\Phi_{\boldsymbol{k}}. \tag{17}$$

Since the interaction with the electric field has been incorporated into the magnon Hamiltonian via an effective gauge potential caused by the AC phase, the nonlinear spin photocurrent can now be handled with standard perturbation theory. The nth-order magnon spin current is calculated via the formula $J^{\alpha,(n)}_s = \int[d\boldsymbol{k}]{\rm Tr}[\rho^{(n)}\hat{J}^\alpha_s]$.

C. Magnon spin photoconductivity tensors

It is instructive to consider the magnon SPGE in ordered ferromagnetic insulators, which is a dc spin photocurrent response

$$J_s = \chi^{\alpha\alpha_1\alpha_2}E^{\alpha_1}(\Omega)E^{\alpha_2}(-\Omega), \tag{18}$$

with Ω being the frequency of the light. The photocurrent response is classified as the linearly polarized LP and CP light-induced currents, and the LP (CP) photocurrent is given by the real symmetric (imaginary antisymmetric) component of the photoconductivity tensor $\eta^{\alpha\alpha_1\alpha_2} = \frac{1}{2}{\rm Re}(\chi^{\alpha\alpha_1\alpha_2}+\chi^{\alpha\alpha_2\alpha_1})[\kappa^{\alpha\alpha_1\alpha_2} = \frac{1}{2}{\rm Im}(\chi^{\alpha\alpha_1\alpha_2}-\chi^{\alpha\alpha_2\alpha_1})]$. We show that $\chi^{\alpha\alpha_1\alpha_2}\propto\epsilon^{\alpha_1 z\beta}\epsilon^{\alpha_2 z\gamma}$ ($\epsilon^{\alpha_2 z\gamma}$ is the Levi-Civita symbol). That is, the electric field is restricted to the plane perpendicular to the axis of magnetization, attributed to the orthogonality between the electric field and the magnon magnetic moment, as illustrated by Eq. (1) and a schematic in Fig. 1(a). For the charge photocurrent, however, there is no such constraint, making it a prominent character. Leaving the details of the calculation in Appendix E, we obtain

$$\chi^{\alpha\alpha_1\alpha_2} = \chi^{\alpha\alpha_1\alpha_2}_{\rm D} + \chi^{\alpha\alpha_1\alpha_2}_{\rm BCD} + \chi^{\alpha\alpha_1\alpha_2}_{\rm Inj} + \chi^{\alpha\alpha_1\alpha_2}_{\rm Sh} + \chi^{\alpha\alpha_1\alpha_2}_{\rm Rec}, \tag{19}$$

with the functional forms of all contributions tabulated in Table I. We denote different contributions as follows: Drude ($\chi^{\alpha\alpha_1\alpha_2}_{\rm D}$), Berry curvature dipole (BCD) ($\chi^{\alpha\alpha_1\alpha_2}_{\rm BCD}$), injection ($\chi^{\alpha\alpha_1\alpha_2}_{\rm Inj}$), shift ($\chi^{\alpha\alpha_1\alpha_2}_{\rm Sh}$), and the rectification current ($\chi^{\alpha\alpha_1\alpha_2}_{\rm Rec}$). Note that in Ref. [14] a magnon shift spin current is proposed that is driven by the magnetic field component of the electromagnetic wave. In contrast, the magnon shift current here manifests as the response of the electric field.

The physical meaning of each contribution in Eq. (19) is schematically shown in Figs. 1(b)–1(d). The Drude-spin current (DSC) arises from the second-order correction to the distribution function and the band gradient velocity, hence it manifests as a pure intraband effect. As with the nonlinear Drude contribution for charge spin current [33,34], the nonlin-

TABLE I. Different terms leading to the magnon SPGE [see Eq. (19)]. The spin photoconductivities are evaluated in terms of the following gauge invariant quantities: group velocity $v_m^\alpha = \frac{1}{\hbar}\partial^\alpha \varepsilon_m$, where $\partial^\alpha = \partial/\partial k_\alpha$; velocity difference $\Delta_{mn}^\alpha = v_m^\alpha - v_n^\alpha$; Berry curvature $\Omega_m^\tau = \epsilon^{\alpha\gamma\tau}\partial^\gamma \mathcal{A}_{nn}^\tau$; band-resolved quantum metric (Berry curvature) $G_{mn}^{\beta\gamma} = \{\mathcal{A}_{mn}^\beta, \mathcal{A}_{nm}^\gamma\}/2$ ($\Omega_{mn}^{\beta\gamma} = i[\mathcal{A}_{mn}^\beta, \mathcal{A}_{nm}^\gamma]$); shift vector $R_{mn}^{\alpha\alpha_1} = \mathcal{A}_{mm}^\alpha - \mathcal{A}_{nn}^\alpha - \partial^\alpha \arg \mathcal{A}_{mn}^{\alpha_1}$; chiral shift vector $R_{mn}^{\alpha,\pm} = \mathcal{A}_{mm}^\alpha - \mathcal{A}_{nn}^\alpha - \partial^\alpha \arg \mathcal{A}_{mn}^\pm$ with the Berry connection in circular representation $\mathcal{A}_{mn}^\pm = \frac{1}{\sqrt{2}}(\mathcal{A}_{mn}^x \pm i\mathcal{A}_{mn}^y)$. $\varsigma = \alpha\Omega = 1/\tau$, where α is the Gilbert damping constant and τ is the relaxation time. The conductivities can be written as $\eta^{\alpha\alpha_1\alpha_2} = (\nu_c/2)\int[d\boldsymbol{k}]\mathcal{I}^{\alpha\alpha_1\alpha_2}$ and $\kappa^{\alpha\alpha_1\alpha_2} = (\nu_c/2)\int[d\boldsymbol{k}]\mathcal{K}^{\alpha\alpha_1\alpha_2}$, with $\mathcal{I}$ and $\mathcal{K}$ being the integrand, and ν_c being the constant $g^2\mu_B^2/(\hbar^2 c^4)$. The symbols ↕ and ↻ denote photocurrents induced by LP and CP light, respectively. Note that the LP responses include a factor $\varsigma = 1$ for $\alpha_1 = \alpha_2$ and $\varsigma = -1$ for $\alpha_1 \neq \alpha_2$. A phenomenological scattering rate Γ is introduced for the injection current.

Current	Spin photoconductivity	$\mathcal{T}'$	$\mathcal{PT}'$	Physical origin
Drude↕	$\mathcal{I}_{\mathrm{D}}^{\alpha\alpha_1\alpha_2} = \varsigma(2/\hbar)\sum_m v_m^\alpha \partial^{\alpha_1}\partial^{\alpha_2} g_m$	×	✓	Nonequilibrium distribution
BCD↻	$\mathcal{K}_{\mathrm{BCD}}^{\alpha\alpha_1\alpha_2} = (\Omega/\hbar)\sum_m(\epsilon^{\alpha\alpha_2\tau}\partial^{\alpha_1} - \epsilon^{\alpha\alpha_1\tau}\partial^{\alpha_2})\Omega_m^\tau g_m$	✓	×	Anomalous velocity + nonequilibrium distribution
Injection↕	$\mathcal{I}_{\mathrm{Inj}}^{\alpha\alpha_1\alpha_2} = -\varsigma 4\hbar\sum_{m,n}\frac{\Omega^2}{(\hbar\Omega-\varepsilon_{mn})^2+\varsigma^2}\Delta_{mn}^\alpha G_{mn}^{\alpha_1\alpha_2} g_{mn}$	×	✓	Velocity difference + dipole transition
Injection↻	$\mathcal{K}_{\mathrm{Inj}}^{\alpha\alpha_1\alpha_2} = -2\pi\hbar\sum_{m,n}\frac{\Omega^2}{(\hbar\Omega-\varepsilon_{mn})^2+\varsigma^2}\Delta_{mn}^\alpha \Omega_{mn}^{\alpha_1\alpha_2} g_{mn}$	✓	×	Velocity difference + dipole transition
Shift↕	$\mathcal{I}_{\mathrm{Sh}}^{\alpha\alpha_1\alpha_2} = \varsigma 2\pi\sum_{m,n}\Omega^2\delta_{\hbar\Omega-\varepsilon_{mn}} R_{mn}^{\alpha\alpha_1} G_{mn}^{\alpha_1\alpha_1} g_{mn}$	✓	×	Position shift + dipole transition
Shift↻	$\mathcal{K}_{\mathrm{Sh}}^{\alpha\alpha_1\alpha_2} = -4\pi\sum_{m,n}\Omega^2\delta_{\hbar\Omega-\varepsilon_{mn}}(R_{mn}^{\alpha,+}\lvert\mathcal{A}_{nm}^+\rvert^2 - R_{mn}^{\alpha,-}\lvert\mathcal{A}_{nm}^-\rvert^2) g_{mn}$	×	✓	Position shift + dipole transition
Rectification↕	$\mathcal{I}_{\mathrm{Rec}}^{\alpha\alpha_1\alpha_2} = \varsigma 4\sum_{m,n}\frac{\Omega^2}{\hbar\Omega-\varepsilon_{mn}} G_{mn}^{\alpha_1\alpha_2}\partial^\alpha g_{mn}$	×	✓	Dipole transition +nonequilibrium distribution
Rectification↻	$\mathcal{K}_{\mathrm{Rec}}^{\alpha\alpha_1\alpha_2} = -\sum_{m,n}\frac{\Omega^2}{\hbar\Omega-\varepsilon_{mn}}\Omega_{mn}^{\alpha_1\alpha_2}\partial^\alpha g_{mn}$	✓	×	Dipole transition +nonequilibrium distribution

ear Drude current for the magnon has an additional symmetry for swapping the current and field direction indices. As a consequence, it is allowed under LP light but is forbidden under the CP light.

Similar to the BCD-resulting nonlinear charge current, the BCD-spin current (BSC) for the magnon originates from a dipole moment of the magnon Berry curvature in momentum space, and it is classified as a CP response. However, contrary to the charge counterpart, the BSC for the magnon scales with the frequency of light and hence vanishes as Ω approaches zero. It is worth noting that the magnon BSC driven by the temperature gradient has been proposed [35], while here we show that there is a BCD contribution as an electric field response, which has not been reported yet.

For the charge case, the shift current due to an instantaneous shift in the charge distribution upon the absorption of light, and the injection current due to the injection of a carrier distribution that is asymmetric in momentum space, have been studied extensively, and they are considered to be the main bulk photovoltaic effect [36–39]. In analogy, we found that the shift-spin current (SSC) for the magnon can be described as a coherent response associated with the real-space shift of a magnon induced by a dipole-mediated vertical interband transition. For LP light response, the shift vector R_{mn}^{α,α_1} recovers the well-known expression as the charge case [40,41], which implies a wave-packet shift of the excited magnons along the α direction through the interband transition $m \leftrightarrow n$. Notably, the chiral shift vector $R_{mn}^{\alpha,\pm}$ characterizes the chirality of the dipole-transition amplitude denoted by $\mathcal{A}_{mn}^\pm$ excited by CP light, resulting in a gyration MSPC. A similar gyration charge current was recently discovered in a magnetically parity-violating system [37].

The injection spin current (ISC) arises from the velocity difference (Δ_{mn}) during the interband transition. It is known that the charge injection current scales linearly with respect to the relaxation time τ and is expected to exhibit a large current response when the electron lifetime is long [38], and it vanishes with strong scattering as $\tau \to 0$. In contrast, we found that the ISC in our proposal remains finite within the limit $\tau \to 0$. It is worth noting that the ISCs proposed are found to be both CP and LP responses.

Finally, the rectification spin currents (RSCs) as both LP and CP responses are demonstrated in this work. They are proportional to the derivatives of the distributions, and they can be regarded as an analog of the "intrinsic Fermi surface effect" in an electronic system [37]. Interestingly, from Table I, it is found that the LP responses (apart from the DSC since it is not geometry-related) are determined by the *band-resolved quantum metric*, while the CP responses are determined by the *Berry curvature*. Our quantum kinetic theory-based treatment of the electric field interaction via the effective dipole interaction provides a complete picture of the magnon SPGE, as summarized in Figs. 1(b)–1(d).

D. Symmetry characters

Since the present method and the developed theory have been proposed, a symmetry analysis is quite useful to outline the scope of this study. For a magnet with collinear magnetic order, it is invariant under the combined symmetry operation of the time-reversal $\mathcal{T}$ and a π spin rotation about the axis perpendicular to the plane of the magnetic order. This is called the effective time-reversal symmetry $\mathcal{T}'$ [42,43]. A general Hamiltonian can be transformed with the effective TRS

TABLE II. Classification on the spin photoconductivities the Drude, BCD, injection, shift, and rectification spin current for LP and CP light by the point-group operation and the effective time-reversal $\mathcal{T}'$. The allowed (forbidden) conductivities are indicated by ✓ (×).

	$\mathcal{P}$	C_2^y	C_2^z	$\mathcal{P}C_2^y$	$\mathcal{P}C_2^z$	C_3^z	C_4^z	$\mathcal{P}C_4^z$	$C_4^z\sigma_v$	$\mathcal{T}'$	$\mathcal{P}\mathcal{T}'$	$C_2^y\mathcal{T}'$	$C_2^z\mathcal{T}'$	$\mathcal{P}C_2^y\mathcal{T}'$	$\mathcal{P}C_2^z\mathcal{T}'$	$C_3^z\mathcal{T}'$	$C_4^z\mathcal{T}'$	$\mathcal{P}C_4^z\mathcal{T}'$	$C_4^z\sigma_v\mathcal{T}'$
$\eta_{\mathrm{D}}^{\alpha\alpha_1\alpha_2}$	×	✓	×	✓	✓	✓	×	×	✓	×	✓	✓	✓	✓	×	×	×	×	×
$\kappa_{\mathrm{BCD}}^{\alpha\alpha_1\alpha_2}$	×	✓	×	✓	✓	×	×	×	✓	✓	×	✓	✓	✓	✓	×	×	×	×
$\eta_{\mathrm{Inj}}^{\alpha\alpha_1\alpha_2}$	×	✓	×	✓	✓	✓	×	×	✓	×	✓	✓	✓	✓	×	×	×	×	×
$\kappa_{\mathrm{Inj}}^{\alpha\alpha_1\alpha_2}$	×	✓	×	✓	✓	×	×	×	✓	✓	×	✓	✓	✓	×	×	×	×	×
$\eta_{\mathrm{Sh}}^{\alpha\alpha_1\alpha_2}$	×	✓	×	✓	✓	✓	×	×	✓	✓	×	✓	✓	✓	✓	×	×	×	×
$\kappa_{\mathrm{Sh}}^{\alpha\alpha_1\alpha_2}$	×	✓	×	✓	✓	×	×	×	✓	×	✓	✓	✓	✓	✓	×	×	×	×
$\eta_{\mathrm{Rec}}^{\alpha\alpha_1\alpha_2}$	×	✓	×	✓	✓	✓	×	×	✓	×	✓	✓	✓	✓	×	×	×	×	×
$\kappa_{\mathrm{Rec}}^{\alpha\alpha_1\alpha_2}$	×	✓	×	✓	✓	×	×	×	✓	✓	×	✓	✓	✓	×	×	×	×	×

operation $\mathcal{T}'$ as

$$\mathcal{T}'\mathcal{H}_{\boldsymbol{k}}(\mathcal{T}')^{-1} = \mathcal{H}_{-\boldsymbol{k}} = \mathcal{H}_{\boldsymbol{k}}^*. \tag{20}$$

It gives rise to

$$U_{\boldsymbol{k}}^\dagger \mathcal{H}_{\boldsymbol{k}} U_{\boldsymbol{k}} = U_{\boldsymbol{k}}^\dagger \mathcal{H}_{-\boldsymbol{k}}^* U_{\boldsymbol{k}} = \mathcal{E}_{\boldsymbol{k}}. \tag{21}$$

Noting that the eigenvalues are real, we have

$$U_{-\boldsymbol{k}}^T \mathcal{H}_{\boldsymbol{k}} U_{-\boldsymbol{k}}^* = (U_{-\boldsymbol{k}}^*)^\dagger \mathcal{H}_{\boldsymbol{k}} U_{-\boldsymbol{k}} = \mathcal{E}_{-\boldsymbol{k}}. \tag{22}$$

The superscript T stands for transpose. Equations (21) and (22) indicate that $U_{\boldsymbol{k}}^\dagger$ and $U_{-\boldsymbol{k}}^*$ differ only by a phase factor matrix, and they share the same eigenvalue equation with $\mathcal{E}_{\boldsymbol{k}} = \mathcal{E}_{-\boldsymbol{k}}$. The element of the Berry connection matrix is

$$\mathcal{A}_{\boldsymbol{k}mn}^\alpha = i\sum_p (U_{\boldsymbol{k}}^\dagger)_{mp} \frac{\partial (U_{\boldsymbol{k}})_{pn}}{\partial k_\alpha} = i\sum_p U_{\boldsymbol{k}pm}^* \frac{\partial U_{\boldsymbol{k}pn}}{\partial k_\alpha}.$$

The $\mathcal{T}'$ symmetry gives a constraint on the Berry connection $\mathcal{A}_{\boldsymbol{k}mn}^\alpha = \mathcal{A}_{-\boldsymbol{k}nm}^\alpha$, and the Berry curvature then satisfies $\Omega_{\boldsymbol{k}m}^\tau = -\Omega_{-\boldsymbol{k}m}^\tau$. Similarly, with $\mathcal{T}'$, the band-resolved Berry curvature, the band-resolved quantum metric, and the shift vector satisfy

$$\Omega_{\boldsymbol{k}mn}^{\alpha\beta} = -\Omega_{-\boldsymbol{k}mn}^{\alpha\beta}, \tag{23}$$

$$G_{\boldsymbol{k}mn}^{\alpha\beta} = G_{-\boldsymbol{k}mn}^{\alpha\beta}. \tag{24}$$

$$R_{\boldsymbol{k}mn}^{\alpha\beta} = R_{-\boldsymbol{k}mn}^{\alpha\beta}. \tag{25}$$

Let us consider the magnon spin photoconductivities. $\eta_{s,\mathrm{Drude}}^{\alpha\alpha_1\alpha_2}$ is $\mathcal{T}'$-odd, indicating that they are finite only when $\mathcal{T}'$ are broken. The integrand of $\kappa_{s,\mathrm{BCD}}^{\alpha\alpha_1\alpha_2}$ transforms as

$$\partial^{\alpha_1}\Omega_{\boldsymbol{k}m}^\tau = \partial^{\alpha_1}\Omega_{-\boldsymbol{k}m}^\tau. \tag{26}$$

It results in $\kappa_{s,\mathrm{BCD}}^{\alpha\alpha_1\alpha_2}$ being $\mathcal{T}'$-even. For the LP injection current $\eta_{s,\mathrm{inj}}^{\alpha\alpha_1\alpha_2}$, we have

$$\Delta_{\boldsymbol{k}mp}^\alpha G_{\boldsymbol{k}mp}^{\beta\gamma} g_{\boldsymbol{k}mp} = -\Delta_{-\boldsymbol{k}mp}^\alpha G_{-\boldsymbol{k}mp}^{\beta\gamma} g_{-\boldsymbol{k}mp}, \tag{27}$$

leading to the LP ISC being odd under $\mathcal{T}'$. Similarly, the integrand of CP ISC $\kappa_{s,\mathrm{inj}}^{\alpha\alpha_1\alpha_2}$ satisfies

$$\Delta_{\boldsymbol{k}mp}^\alpha \Omega_{\boldsymbol{k}mp}^{\beta\gamma} g_{\boldsymbol{k}mp} = \Delta_{-\boldsymbol{k}mp}^\alpha \Omega_{-\boldsymbol{k}mp}^{\beta\gamma} g_{-\boldsymbol{k}mp}, \tag{28}$$

i.e., the CP ISC is $\mathcal{T}'$-even. For the LP SSC $\eta_{s,\mathrm{shift}}^{\alpha\alpha_1\alpha_1}$, the integrand satisfies

$$R_{\boldsymbol{k}mn}^{\alpha_1\alpha_1} G_{\boldsymbol{k}mn}^{\alpha_1\alpha_1} g_{\boldsymbol{k}mn} = R_{-\boldsymbol{k}mn}^{\alpha_1\alpha_1} G_{-\boldsymbol{k}mn}^{\alpha_1\alpha_1} g_{-\boldsymbol{k}mn}, \tag{29}$$

suggesting that $\eta_{s,\mathrm{shift}}^{\alpha\alpha_1\alpha_2}$ is $\mathcal{T}'$-even. The CP SSC $\kappa_{s,\mathrm{shift}}^{\alpha\alpha_1\alpha_2}$ is justified to be $\mathcal{T}'$-odd in a similar way. In analogy, the LP RSC $\eta_{s,\mathrm{rect}}^{\alpha\alpha_1\alpha_1}$ is $\mathcal{T}'$-odd and the CP RSC $\kappa_{s,\mathrm{rect}}^{\alpha\alpha_1\alpha_2}$ is $\mathcal{T}'$-even.

Now we consider the point-group symmetry transformations. With a point-group symmetry $\mathcal{M}$, the eigenvalues satisfy $\varepsilon_{n\boldsymbol{k}} = \varepsilon_{n\mathcal{M}^{-1}\boldsymbol{k}}$, and the Berry connection transforms as

$$\mathcal{A}_{\boldsymbol{k}mn}^\alpha = \mathcal{M}_{\alpha\beta}\mathcal{A}_{\mathcal{M}^{-1}\boldsymbol{k}mn}^\beta. \tag{30}$$

The derivative operation transforms as

$$\frac{\partial g_{\boldsymbol{k}m}}{\partial \boldsymbol{k}_\alpha} = \mathcal{M}_{\alpha\beta}\frac{\partial g_{\mathcal{M}^{-1}\boldsymbol{k}m}}{\partial \boldsymbol{k}_\beta}. \tag{31}$$

From these properties, for a general conductivity tensor, one can find that

$$\chi^{\alpha'\alpha_1'\alpha_2'} = \mathcal{M}^{\alpha'\alpha}\mathcal{M}^{\alpha_1'\alpha_1}\mathcal{M}^{\alpha_2'\alpha_2}\chi^{\alpha\alpha_1\alpha_2}. \tag{32}$$

For a CP response tensor, it is antisymmetric by permuting the last two indices, and it is convenient to transform it to an equivalent rank-2 pseudotensor

$$\varpi^{\alpha\beta} = \epsilon^{\beta\alpha_1\alpha_2}\kappa^{\alpha\alpha_1\alpha_2}/2, \tag{33}$$

and the operation of $\mathcal{M}$ yields

$$\varpi^{\alpha'\beta'} = \det(\mathcal{M})\mathcal{M}^{\alpha'\alpha}\mathcal{M}^{\beta'\beta}\varpi^{\alpha\beta}. \tag{34}$$

The constraints on the in-plane magnon spin photoconductivity tensors from the point-group symmetries and the effective time-reversal $\mathcal{T}'$ are listed in Table II. It is seen that the existence of the magnon spin current requires either $\mathcal{T}'$ or $\mathcal{P}\mathcal{T}'$ symmetry to be broken. For example, the Drude contribution is forbidden by $\mathcal{T}'$, while the Berry curvature dipole contribution is forbidden by $\mathcal{P}\mathcal{T}'$. Further constraints on the magnon spin currents are introduced by the point group symmetries. For example, the C_{3z} symmetry forces all the circularly-polarized-light responses of the magnon spin current to vanish.

III. RESULTS

A. Application to breathing kagome ferromagnet

The breathing kagome lattice has gained growing interest in studies of the quantum spin liquid [44–49]. To illustrate the proposed magnon spin photogalvanic effect, we study a breathing kagome-lattice ferromagnet in the absence of inversion symmetry, as shown in Fig. 2(a). With a nonuniform strain field, the three sublattices are deformed farther

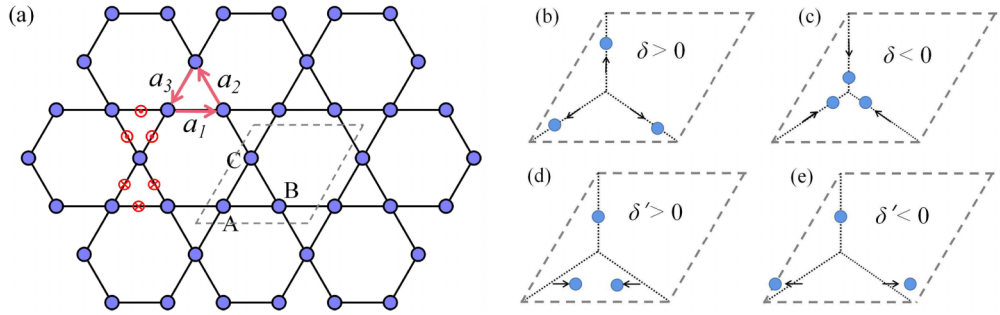

FIG. 2. (a) Schematics for the kagome ferromagnet with lattice constant a. The NN vectors are labeled by a_i. Sublattices A, B, and C are placed at the corners of the triangles. Dzyaloshinskii-Moriya vectors are aligned normal to the lattice plane, and their directions (up and down) are represented by the symbols $\odot$ and $\otimes$, depending on the chirality of the triangles. The dashed lines represent a unit cell. (b),(c) Strain is introduced by letting the sublattice be farther away ($\delta > 0$) or closer ($\delta < 0$).

away (positive perturbation $\delta > 0$) or getting closer (negative perturbation $\delta < 0$) from their shared corner, as shown in Figs. 2(b) and 2(c). The Hamiltonian is

$$H = -\sum_{\langle i,j\rangle} J_{ij}\boldsymbol{S}_i \cdot \boldsymbol{S}_j + \sum_{\langle i,j\rangle} \boldsymbol{D}_{ij} \cdot \boldsymbol{S}_i \times \boldsymbol{S}_j. \tag{35}$$

$J > 0$ is the nearest-neighbor (NN) ferromagnetic coupling strength. The second term is the out-of-plane NN Dzyaloshinskii-Moriya interaction (DMI); the Dzyaloshinskii-Moriya (DM) vector is specified as $\boldsymbol{D}_{ij} = v_{ij}D\boldsymbol{z}$ with $v_{ij} = \pm$, depending on the chirality of the triangles in the kagome lattice. The ferromagnetic exchange interaction and the DMI are given by [48,50] $J_\pm = (1 \mp \sqrt{3}\eta\delta)J$, $D_\pm = (1 \mp \sqrt{3}\eta\delta)D$, where subscript $+$ $(-)$ denotes intracell (intercell) NN couplings, η is a parameter describing the response of the couplings to the displacements of sublattices, and δ is the strain parameter. The bosonic Hamiltonian can be derived as $\mathcal{H}_{\boldsymbol{k}} = \mathcal{H}_0 - \mathcal{H}_J^{\rm NN} - \mathcal{H}_{\rm DM}$, where $\mathcal{H}_0 = 4JI_{3\times3}$. The nearest-neighbor magnetic exchange coupling reads

$$\mathcal{H}_J^{\rm NN} = \begin{pmatrix} 0 & \gamma_2 & \gamma_3^* \\ \gamma_2^* & 0 & \gamma_1 \\ \gamma_3 & \gamma_1^* & 0 \end{pmatrix},$$
$$\mathcal{H}_{\rm DM} = i\begin{pmatrix} 0 & d_1 & -d_3^* \\ -d_1^* & 0 & d_2 \\ d_3 & -d_2^* & 0 \end{pmatrix}, \tag{36}$$

with $\gamma_i = J_+ e^{i\boldsymbol{k}\cdot(1+\delta)\boldsymbol{a}_i} + J_- e^{-i\boldsymbol{k}\cdot(1-\delta)\boldsymbol{a}_i}$ and $d_i = D_+ e^{i\boldsymbol{k}\cdot(1+\delta)\boldsymbol{a}_i} + D_- e^{-i\boldsymbol{k}\cdot(1-\delta)\boldsymbol{a}_i}$.

Different topological phases are characterized by sets of Chern numbers (C_1, C_2, C_3) of the lower, middle, and upper magnon bulk bands. A topological phase transition has been discovered by tuning δ [50]. Figure 3(a) shows the magnon bulk bands along the high-symmetry directions (Γ-K-M-Γ) of the Brillouin zone. For $\delta = 0$ the topological phase is $(-1, 0, 1)$, and for $\delta = 0.1$ the topological phase is $(0, -1, 1)$. A topological phase transition occurs at $\delta_c = 0.05$, where the two magnon branches cross linearly at the K point.

The DMI breaks the effective $\mathcal{T}'$ symmetry, and it also reduces the C_{6z} symmetry to C_{3z}, yet it preserves the C_{2x} symmetry. Then both of the LP and CP responses are forbidden. It is worth noting that the breathing geometry preserves the C_{3z} symmetry and breaks C_{2x}, hence all the CP responses are forbidden but the LP responses are allowed. In Fig. 3(b) we show the magnon spin photoconductivities η^{xxx} of the allowed injection, rectification, and shift spin current in response of the LP light, varying with the lattice deformation. For $\delta = 0$, the LP responses are zero due to the C_{2x} symmetry. As δ increases, finite LP responses appear as required by symmetry. The $(-1, 0, 1)$ phase and the $(0, -1, 1)$ phase are separated by the critical points of the phase transition represented by the dashed black lines. Remarkably, both the injection and the rectification spin current exhibit a peak at the critical point, while the derivative of the shift spin current maximizes at the critical point. As for the DSC, there is no such drastic change at the critical point, because the DSC is exclusively determined by the group velocities and their derivatives, which is independent of the magnon topology. This clearly indicates a topological phase transition that is also manifested as a plateau of the total LP photoconductivity at the critical point, which can serve as a prominent indicator to determine the topological phase transition in experiments.

A breathing kagome-lattice ferromagnet preserves the C_{3z} symmetry, hence all the CP responses are forbidden. Now we consider an additional uniaxial strain along the x-axis breaking the C_{3z} symmetry, for which the spins along the x-axis are pushing closer, $\delta' > 0$, or farther, $\delta' < 0$, as shown in Figs. 2(d) and 2(e). The remaining point-group symmetry is σ_x, for which the CP responses are allowed. In the presence of δ', the diagonal component $\mathcal{H}_0$ is modified as $\mathcal{H}_0 = J\,\mathrm{diag}(4, 2(2+\delta'), 2(2+\delta'))$. For $\mathcal{H}_J^{\rm NN}$, only the (1,2) and (2,1) elements are changed to $\gamma_2' = (1+\delta')\gamma_2$ [51]. By increasing δ' from zero, a topological phase transition occurs at the critical point $\delta_c' = \frac{1}{2}[1 - (D/J)^2]$, where the upper band and the middle band cross at the M point. In Fig. 3(c) we show the magnon bands along the high-symmetry points for different δ' but with fixed $\delta = 0.02$ (and $D/J = 0.2$). Similar to Ref. [51], a topological phase transition occurs when the system is tuned from the $(-1, 0, 1)$-phase to the $(-1, 1, 0)$-phase by increasing δ', while the critical point is found at $\delta_c' = 0.54$. In Fig. 3(d) we show the CP spin conductivities κ_s^{xyx} as functions of δ', where we set the circular polarization of light to be in the xy plane, and we measure the z-direction spin current. One observes that all four kinds of CP responses change abruptly at $\delta' = \delta_c'$, indicating a topological magnon phase transition, which is a direct manifestation of the change

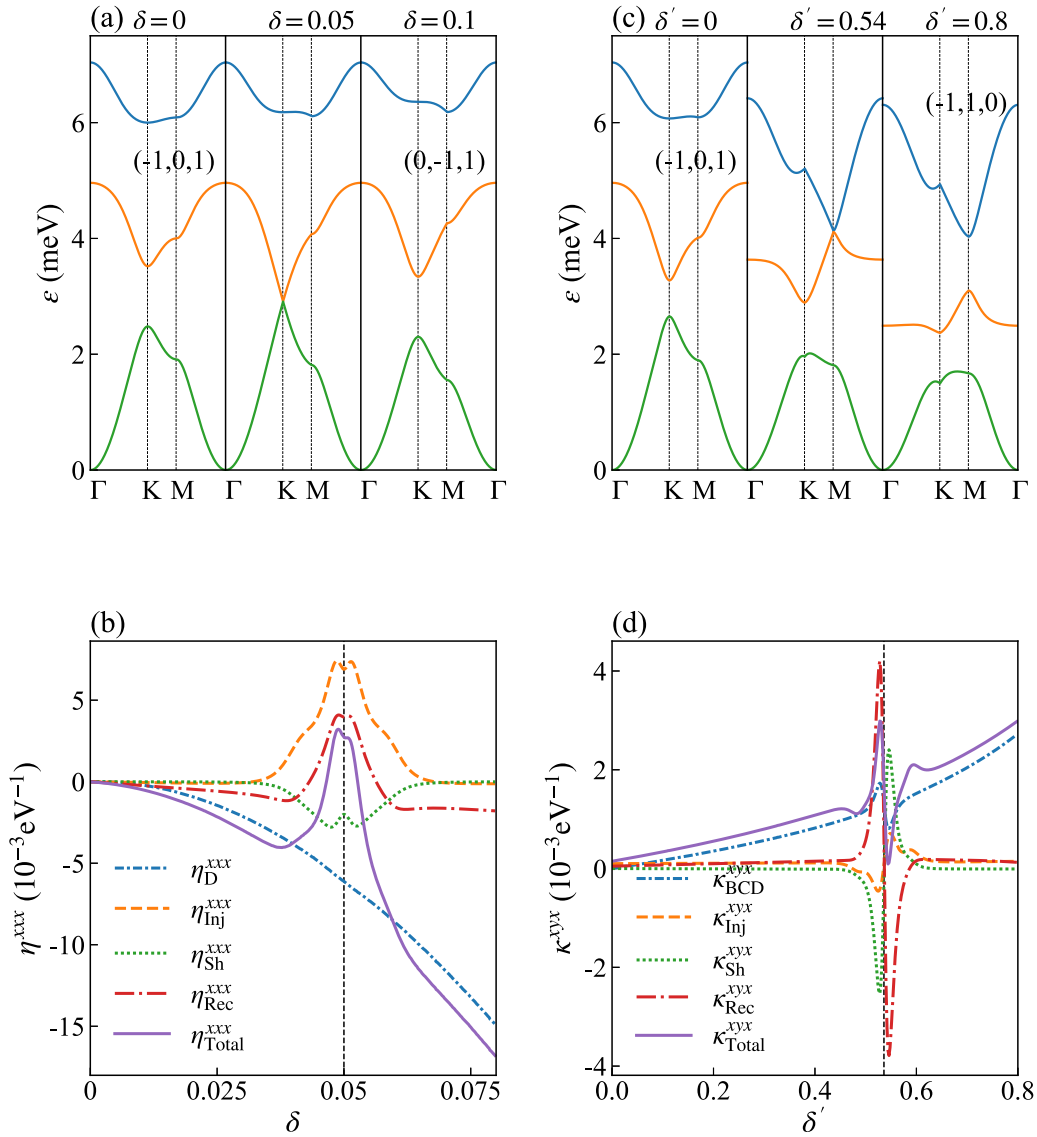

FIG. 3. (a) Magnon band structures of a breathing kagome-lattice ferromagnet with different lattice deformation δ. Considering that $\delta > 0$ and $\delta < 0$ are equivalent, only cases $\delta > 0$ are plotted. (b) LP photoconductivities as a function of the lattice deformation. The critical point of the phase transition is shown as a vertical dashed line. (c) Magnon band structures of a breathing kagome-lattice ferromagnet in the presence of $\delta = 0.02$ with different uniaxial strain δ'. The critical point is $\delta' = 0.54$. (d) The CP photoconductivities vs the uniaxial strain δ', where the critical point of the phase transition is shown as a vertical dashed line. Parameters are set as $J = 3.405$, $D = 1.02$, $\hbar\Omega = 0.15$ in units of meV. Gilbert damping constant α is estimated as $\alpha = 10^{-2}$, temperature is $T = 50$ K.

of the topological properties, such as the Berry curvature and the shift vector in momentum space.

B. Materials realization

In the previous section, we qualitatively analyze the response tensors by symmetry, and we characterize the behavior near the phase-transition point. Now we consider the magnitude for the magnon spin photoconductivity. The candidate materials can be the three-dimensional (3D) ferromagnetic pyrochlore oxides $Lu_2V_2O_7$, $In_2Mn_2O_7$, as well as $Ho_2V_2O_7$ [8], with a nonuniform strain applied. Instead of considering a true 3D lattice, we can realize our idea by treating the system as a stack of noninteracting (or weakly interacting) kagome layers. Here we consider the $Lu_2V_2O_7$ with nonuniform strain applied. The lattice constant is $a = 7.024$ Å and the Curie temperature is 70 K [8]. The nearest Heisenberg interaction is estimated as $J_1 = 3.405$ meV [52], and we set the temperature to $T = 50$ K with a ferromagnetic ground state. From these values and our numerical result in Figs. 3(c) and 3(d), we obtain that the total magnon spin photoconductivity under the LP and CP light can reach 10^{-2} e/V near the phase-transition points. When applying an ac electric field of $E \sim 10^3$ V/m, it leads to a magnon spin current $J_s \sim 10^{-2}$ eV/cm^2, which is experimentally detectable. The generated magnon spin current can be detected via the inverse spin Hall effect [53].

Though the AC phase scales with $1/c^2$, the obtained observable magnon spin currents induced by the AC phase can be understood as follows. We can compare the AC-phase-resulting magnon spin currents to electron

spin currents in response to the electric field. To be specific, suppose that we consider a circularly polarized laser (electromagnetic) field with the electric field component $\boldsymbol{E}(t) = E_0(\cos\omega t, \sin\omega t, 0)$. With use of $\boldsymbol{E}(t) = -\partial_t A(t)$, the magnetic vector potential is written as $\boldsymbol{A}(t) = A_0(\sin\omega t, -\cos\omega t, 0)$. The AC phase is given by $\theta_{ij}^{\mathrm{AC}} = \frac{g\mu_B}{\hbar c^2}\int_{\boldsymbol{r}_i}^{\boldsymbol{r}_j}[\boldsymbol{E}(t)\times\hat{\boldsymbol{e}}_z]\cdot d\boldsymbol{r}$, which can be rewritten as $\theta_{ij}^{\mathrm{AC}} = \frac{g\mu_B\omega}{\hbar c^2}\int_{\boldsymbol{r}_i}^{\boldsymbol{r}_j}[\boldsymbol{A}(t+\frac{\pi}{2\omega})\times\hat{\boldsymbol{e}}_z]\cdot d\boldsymbol{r}$. As is known, the Aharonov-Bohm phase is $\theta_{ij}^{\mathrm{AB}} = \frac{q}{\hbar}\int_{\boldsymbol{r}_i}^{\boldsymbol{r}_j}\boldsymbol{A}(t)\cdot d\boldsymbol{r}$. This means that for the same vector potential $\boldsymbol{A}$ or electric field $\boldsymbol{E}$, there is a relation $\theta_{ij}^{\mathrm{AC}}/\theta_{ij}^{\mathrm{AB}} \sim g\mu_B\omega/qc^2$, implying a considerable AC effect with large ω. For example, a 100 THz electric field yields $g\mu_B\omega/qc^2 \sim 10^{-6}$. Consequently, when increasing the electric field to three orders larger (considering that the magnon spin photogalvanic effect is of the second-order response), the magnitude of the magnon spin current can approach that of the charge spin current case.

Note that the intrinsic (without nonuniform strain) breathing kagome ferromagnet has been synthesized in rare-earth-based pyrochlore materials such as $Ba_3Yb_2Zn_55O_{11}$ [54] as well as $LiZn_2Mo_3O_8$ [55]. Also, a field-aligned ferromagnetic phase was experimentally observed in the centrosymmetric breathing kagome lattice $Gd_3Ru_4Al_{12}$ [56]. We expect that the MSPC we proposed can be observed in these candidate materials. With symmetry analysis, this study can be naturally extended to other materials by using the magnetic structure database MAGNDATA [57].

IV. DISCUSSION AND CONCLUSION

To conclude, we proposed a magnon spin photogalvanic effect, and we uncovered the geometric origin due to an AC phase accumulation. It provides a mechanism for the optical (electric) generation and control of the magnons. Because the electric component of light is of a wide, tunable parameter scale and is very fast, this method may have a realistic platform in applications. We further identify five new mechanisms: Drude, BCD, injection, shift, and rectification spin current. It is found that the linearly-polarized-light responses (except Drude) are determined by the band-resolved quantum metric, while the circularly-polarized-light responses are determined by the Berry curvature. In general, the magnon does not conserve spin angular momentum in processes such as the dipolar interaction [58] and the magnon-magnon interaction, which involve the pair creation and annihilation of magnons, as well as scattering with magnetic impurity, which disturbs the magnon spin angular momentum [59]. Here we assume that the Heisenberg exchange coupling is strong enough to suppress the dipolar interaction [60], the temperature is low, and the impurities are sufficiently sparse that the magnon-magnon interaction and impurity scattering are negligible [61]. We can then restrict the study to a situation in which the magnon preserves the spin angular momentum $\pm\hbar$ when it transfers among sites; we leave the generalization in which the magnon does not conserve the spin angular momentum for future study. Finally, we emphasize that the present calculation is also valid for the case of an ac bias applied to the sample, and it may be of great interest to experimenters.

ACKNOWLEDGMENTS

This work is supported by the National Key R&D Program of China (Grant No. 2022YFA1402802). It is also supported in part by the NSFC (Grants No. 11974348 and No. 11834014), and the Strategic Priority Research Program of CAS (Grants No. XDB28000000 and No. XDB33000000). Z.G.Z. is supported in part by the Training Program of Major Research plan of the National Natural Science Foundation of China (Grant No. 92165105) and CAS Project for Young Scientists in Basic Research Grant No. YSBR-057.

APPENDIX A: LINEAR SPIN-WAVE THEORY AND MAGNON HAMILTONIAN

Here we rewrite the general two-body spin interaction Hamiltonian,

$$H = \frac{1}{2}\sum_{i,j}^{L}\sum_{n,m}^{N}\sum_{\alpha\beta} S_{i,n}^{\alpha}H_{nm}^{\alpha\beta}(i-j)S_{j,m}^{\beta}. \tag{A1}$$

By setting global (reference) coordinates $(\hat{\boldsymbol{x}}, \hat{\boldsymbol{y}}, \hat{\boldsymbol{z}})$, the local coordinates (spherical coordinates) of each spin are related to the global coordinates via

$$\boldsymbol{S}_{i,n} = R_n(\theta_i, \phi_i)\boldsymbol{S}_0. \tag{A2}$$

The classical ground state is identified by treating the quantum-mechanical spin operators as classical vectors and minimizing the classical ground-state energy. The magnons have the usual low-energy excitation in ordered magnets, which is considered via the Holstein-Primakoff transformation in local coordinates [25,62],

$$\begin{aligned} S_{i,n}^{\theta} &= \sqrt{\frac{S}{2}}(a_{i,n} + a_{i,n}^{\dagger}), \\ S_{i,n}^{\phi} &= -i\sqrt{\frac{S}{2}}(a_{i,n} - a_{i,n}^{\dagger}), \\ S_{i,n}^{r} &= S - a_{i,n}^{\dagger}a_{i,n}, \end{aligned} \tag{A3}$$

and we obtain

$$\boldsymbol{S}_{i,n}^{\alpha} = \sqrt{\frac{S}{2}}\hat{\boldsymbol{u}}_n a_{i,n} + \sqrt{\frac{S}{2}}\hat{\boldsymbol{u}}_n^{*}a_{i,n}^{\dagger} + \hat{\boldsymbol{z}}_n(S - a_{i,n}^{\dagger}a_{i,n}), \tag{A4}$$

where $\alpha = x, y, z$. The coefficients $\hat{\boldsymbol{u}}_n$ and $\hat{\boldsymbol{z}}_n$ are related to the relative rotation between the global and local coordinates, which are written explicitly as

$$\begin{aligned} \begin{pmatrix} u_n^x \\ u_n^y \\ u_n^z \end{pmatrix} &= \begin{pmatrix} \cos\theta_n\cos\phi_n + i\sin\phi_n \\ \cos\theta_n\cos\phi_n - i\sin\phi_n \\ -\sin\theta_n \end{pmatrix}, \\ \begin{pmatrix} z_n^x \\ z_n^y \\ z_n^z \end{pmatrix} &= \begin{pmatrix} \sin\theta_n\cos\phi_n \\ \sin\theta_n\sin\phi_n \\ \cos\theta_n \end{pmatrix}. \end{aligned} \tag{A5}$$

Expanding the coupling interaction, we obtain

$$\begin{aligned} S_{i,n}^{\alpha}S_{j,m}^{\beta} = {} & \tfrac{1}{2}u_n^{\alpha *}a_{i,n}^{\dagger}\left(u_m^{\beta}a_{j,m} + u_m^{\beta *}a_{j,m}^{\dagger}\right) \\ & + \tfrac{1}{2}u_n^{\alpha}a_{i,n}\left(u_m^{\beta *}a_{j,m}^{\dagger} + u_m^{\beta}a_{j,m}\right) \\ & - z_n^{\alpha}z_m^{\beta}\left(a_{i,n}^{\dagger}a_{i,n} + a_{j,m}^{\dagger}a_{j,m}\right). \end{aligned} \tag{A6}$$

By inserting Eq. (A6) into Eq. (A1), we have

$$\begin{aligned} H =& \sum_{i,j,n,m} A_{nm}(i-j)a^{\dagger}_{i,n}a_{j,m} \\ &+ \frac{1}{2}\sum_{i,j,n,m}[B_{nm}(i-j)a^{\dagger}_{i,n}a^{\dagger}_{j,m} + \text{H.c.}] \\ &+ 2\sum_{i,n,m} C_{nm}a^{\dagger}_{i,n}a_{i,n}, \end{aligned} \tag{A7}$$

in which

$$\begin{aligned} A_{nm}(i-j) &= \frac{\sqrt{S_nS_m}}{2}\sum_{\alpha\beta} u^{\alpha *}_n H^{\alpha\beta}_{nm}(i-j)u^{\beta}_m, \\ B_{nm}(i-j) &= \frac{\sqrt{S_nS_m}}{2}\sum_{\alpha\beta} u^{\alpha *}_n H^{\alpha\beta}_{nm}(i-j)u^{\beta *}_m, \\ C_{nm} &= \delta_{nm}S_l\sum_{\alpha\beta} z^{\alpha}_n \sum_j\sum_l H^{\alpha\beta}_{nm}(i-j)z^{\beta}_l. \end{aligned} \tag{A8}$$

By transforming Eq. (A6) to the reciprocal space, we have

$$a_{i,n} = (1/\sqrt{L})\sum_{\boldsymbol{k}} \exp[i\boldsymbol{k}\cdot(\boldsymbol{r}_i+\boldsymbol{t}_n)]a_{\boldsymbol{k},n}, \tag{A9}$$

where $\boldsymbol{r}_i$ is the position of the ith unit cell, and $\boldsymbol{t}_m$ is the relative vector of the mth sublattice. We have $H = \frac{1}{2}\sum_{\boldsymbol{k}} \Psi^{\dagger}_{\boldsymbol{k}}\mathcal{H}(\boldsymbol{k})\Psi_{\boldsymbol{k}}$, where

$$\mathcal{H}(\boldsymbol{k}) = \begin{pmatrix} A(\boldsymbol{k}) - C & B(\boldsymbol{k}) \\ B^{\dagger}(\boldsymbol{k}) & A^{T}(-\boldsymbol{k}) - C \end{pmatrix} \tag{A10}$$

is a $2N\times 2N$ bosonic Bogoliubov–de Gennes (BdG) Hamiltonian with a vector boson operator, where $\Psi^{\dagger}_{\boldsymbol{k}} = (a^{\dagger}_{\boldsymbol{k},1},\ldots,a^{\dagger}_{\boldsymbol{k},N},a_{-\boldsymbol{k},1},\ldots,a_{-\boldsymbol{k},N})$, and the $N\times N$ block matrix is given by

$$\begin{aligned} A_{mn}(\boldsymbol{k}) &= \sum_{\alpha,\beta} u^{\alpha *}_n\left[\sum_{\boldsymbol{d}} e^{-i\boldsymbol{k}\cdot\boldsymbol{d}}H^{\alpha\beta}_{nm}(\boldsymbol{d})\right]u^{\beta}_m, \\ B_{mn}(\boldsymbol{k}) &= \sum_{\alpha,\beta} u^{\alpha *}_n\left[\sum_{\boldsymbol{d}} e^{-i\boldsymbol{k}\cdot\boldsymbol{d}}H^{\alpha\beta}_{nm}(\boldsymbol{d})\right]u^{\beta *}_m, \\ C_{mn} &= \delta_{mn}\sum_{\alpha,\beta}\sum_l z^{\alpha *}_n\left[\sum_{\boldsymbol{d}} H^{\alpha\beta}_{nl}(\boldsymbol{d})\right]z^{\beta}_l, \end{aligned} \tag{A11}$$

where $\boldsymbol{d} = (\boldsymbol{r}_i+\boldsymbol{t}_n) - (\boldsymbol{r}_j-\boldsymbol{t}_m)$ is the difference vector between the mth and the nth spin. In deriving Eq. (A11), the relation

$$\sum_{\boldsymbol{k}}\sum_{n,m} A_{nm}(\boldsymbol{k})a^{\dagger}_{\boldsymbol{k},n}a_{\boldsymbol{k},m} = \sum_{\boldsymbol{k}}\sum_{n,m} A^{T}_{nm}(-\boldsymbol{k})a_{-\boldsymbol{k},n}a^{\dagger}_{-\boldsymbol{k},m} \tag{A12}$$

is used. For collinear ferromagnets, the Hamiltonian Eq. (A10) is block-diagonal with an identical block, which can be reduced to $H = \sum_{\boldsymbol{k}}\Psi_{\boldsymbol{k}}\mathcal{H}_{\boldsymbol{k}}\Psi_{\boldsymbol{k}}$ with $\mathcal{H}_{\boldsymbol{k}} = (A_{\boldsymbol{k}} - C)$ and $\Psi^{\dagger}_{\boldsymbol{k}} = (a^{\dagger}_{\boldsymbol{k},1},\ldots,a^{\dagger}_{\boldsymbol{k},N})$.

APPENDIX B: PERTURBATION OF ELECTRIC FIELD IN THE FORM OF MINIMAL COUPLING

Now we consider the AC effect. In Eq. (A6), the first two terms describe the magnon hopping. In the presence of an electric field, the magnon acquires a phase while traveling between the mth and the nth spin on the ith and jth site, which is given by

$$\theta_{in,jm} = -\frac{g\mu_B}{\hbar c^2}\int_{\boldsymbol{r}_{i,n}}^{\boldsymbol{r}_{j,m}}[\boldsymbol{E}(t)\times\hat{\boldsymbol{e}}_n]\cdot d\boldsymbol{r}. \tag{B1}$$

Note that Eq. (B1) is general despite the dependence of the local coordinates on each site. To see this, let us recall the original expression of the AC phase, $\theta^{\text{AC}}_{ij} = \frac{1}{\hbar c^2}\int_{\boldsymbol{r}_i}^{\boldsymbol{r}_j}[\boldsymbol{E}(t)\times\boldsymbol{\mu}]\cdot d\boldsymbol{r}$, with $\boldsymbol{\mu}$ being the magnetic moment of the magnon. If the direction and magnitude of the magnon magnetic moment do not change during the hopping processes (i.e., we neglect the magnon scattering that involves the angular momentum transfer), then θ^{AC}_{ij} is determined by the distance between the sites once the magnetic ground state is fixed, irrespective of the local coordinates. Similar demonstrations can be found in Refs. [30] and [63]. The coupling interaction is modified as

$$\begin{aligned} S^{\alpha}_{i,n}S^{\beta}_{j,m} =& \tfrac{1}{2}U^{\alpha *}_n a^{\dagger}_{i,n}\left(U^{\beta}_m a_{j,m} + U^{\beta *}_m a^{\dagger}_{j,m}\right)e^{i\theta_{in,jm}} \\ &+ \tfrac{1}{2}U^{\alpha}_n a_{i,n}\left(U^{\beta *}_m a^{\dagger}_{j,m} + U^{\beta}_m a_{j,m}\right)e^{-i\theta_{in,jm}} \\ &- V^{\alpha}_n V^{\beta}_m(a^{\dagger}_{i,n}a_{i,n} + a^{\dagger}_{j,m}a_{j,m}). \end{aligned} \tag{B2}$$

If the scale of the spatial variance of $\boldsymbol{E}$ is much larger than the lattice constant, and introducing the effective vector potential $\boldsymbol{A}^E_n = \frac{1}{c}\boldsymbol{E}\times\hat{\boldsymbol{e}}_n$, one obtains

$$\theta_{in,jm} = \frac{g\mu_B}{\hbar c}\boldsymbol{A}^E_n\cdot\boldsymbol{d}. \tag{B3}$$

Following the same procedure, we have

$$\begin{aligned} A_{nm}(\boldsymbol{k}) &\to A_{nm}\left(\boldsymbol{k} - \frac{g\mu_B}{\hbar c}\boldsymbol{A}^E_n\right), \\ B_{nm}(\boldsymbol{k}) &\to B_{nm}\left(\boldsymbol{k} - \frac{g\mu_B}{\hbar c}\boldsymbol{A}^E_n\right), \end{aligned} \tag{B4}$$

while the matrix C_{nm} is unchanged because there is no magnon hopping involved.

Now we consider two special cases, namely the collinear ferromagnet and the collinear antiferromagnet.

1. Collinear ferromagnet

For ferromagnets, due to the absence of the magnon pairing $a^{\dagger}_{i,n}a^{\dagger}_{j,m}$ and $a_{i,n}a_{j,m}$, the $2N$-dimensional basis is reduced to N-dimensional $\Psi^{\dagger}_{\boldsymbol{k}} = (a^{\dagger}_{\boldsymbol{k},1},\ldots,a^{\dagger}_{\boldsymbol{k},N})$. Accordingly, the Hamiltonian Eq. (A10) is reduced to $\mathcal{H}_{\boldsymbol{k}} = A(\boldsymbol{k}) - C$. It is obvious that the global coordinates are the same as the local coordinates for each spin, which can be chosen such that the z-direction is identical to the magnetization direction. In that regard, the magnetic moment of a magnon is $-\hbar\hat{\boldsymbol{e}}_z$, and the effective vector potential is $\boldsymbol{A}^E_n = \boldsymbol{A}^E = \frac{1}{c}\boldsymbol{E}\times\hat{\boldsymbol{e}}_z$. Consequently, the kernel Hamiltonian becomes $\mathcal{H}(\boldsymbol{k}) = A(\boldsymbol{k} - \frac{g\mu_B}{\hbar c}\boldsymbol{A}^E) - C$.

2. Collinear antiferromagnet

To be specific, we consider a collinear antiferromagnet honeycomb lattice that has two spins in a unit cell, with the Hamiltonian given by

$$H = J_1 \sum_{\langle i,j\rangle} \boldsymbol{S}_i \cdot \boldsymbol{S}_j + D \sum_{\langle\langle ij\rangle\rangle} \xi_{ij} \hat{\boldsymbol{z}} \cdot \boldsymbol{S}_i \times \boldsymbol{S}_j + K \sum_i S_{iz}^2, \quad \text{(B5)}$$

where $J_1 > 0$ is the antiferromagnetic exchange interaction, D is the DMI interaction along the z direction, and $\xi_{ij} = 1\ (-1)$ when $\boldsymbol{S}_i$ and $\boldsymbol{S}_j$ are arranged in a counterclockwise (clockwise) manner. $K < 0$ is the easy-axis anisotropy. One can choose the local coordinates of the first spin of the unit cell as the global coordinates, while the local coordinates of the second spin are obtained by a π rotation about the x-axis or y-axis of the global coordinates. Subsequently, the HP transformation is performed as

$$\begin{aligned} \boldsymbol{S}_{i,1}^{\alpha} &= \sqrt{\frac{S}{2}} \hat{\boldsymbol{u}}_1 a_{i,1} + \sqrt{\frac{S}{2}} \hat{\boldsymbol{u}}_1^* a_{i,1}^\dagger + \hat{\boldsymbol{z}}_1 (S - a_{i,1}^\dagger a_{i,1}), \\ \boldsymbol{S}_{i,2}^{\alpha} &= \sqrt{\frac{S}{2}} \hat{\boldsymbol{u}}_2 a_{i,2} + \sqrt{\frac{S}{2}} \hat{\boldsymbol{u}}_2^* a_{i,2}^\dagger + \hat{\boldsymbol{z}}_2 (S - a_{i,2}^\dagger a_{i,2}), \end{aligned} \quad \text{(B6)}$$

where

$$\begin{aligned} \begin{pmatrix} u_1^x \\ u_1^y \\ u_1^z \end{pmatrix} &= \begin{pmatrix} 1 \\ -i \\ 0 \end{pmatrix}, \quad \begin{pmatrix} z_1^x \\ z_1^y \\ z_1^z \end{pmatrix} = \begin{pmatrix} 0 \\ 0 \\ 1 \end{pmatrix}, \\ \begin{pmatrix} u_2^x \\ u_2^y \\ u_2^z \end{pmatrix} &= \begin{pmatrix} 1 \\ i \\ 0 \end{pmatrix}, \quad \begin{pmatrix} z_2^x \\ z_2^y \\ z_2^z \end{pmatrix} = \begin{pmatrix} 0 \\ 0 \\ -1 \end{pmatrix}. \end{aligned} \quad \text{(B7)}$$

Therefore, the magnon Hamiltonian is $H = H^J + H^D + H^K$, with

$$\begin{aligned} H^J &= J_1 S \sum_{\langle i,j\rangle} (a_{i,1} a_{j,2} + a_{i,1}^\dagger a_{j,2}^\dagger), \\ H^D &= -\sum_{\langle\langle i,j\rangle\rangle} iD_2 S (a_{i,1}^\dagger a_{j,1} - a_{j,1}^\dagger a_{i,1} - a_{i,2}^\dagger a_{j,2} + a_{j,2}^\dagger a_{i,2}), \\ H^K &= \sum_i (3J_1 - K) S (a_{i,1}^\dagger a_{i,1} + a_{i,2}^\dagger a_{i,2}). \end{aligned} \quad \text{(B8)}$$

The operator $a_{i,1}$ ($a_{i,1}^\dagger$) annihilates (creates) a magnon with magnetic moment $-\hbar\hat{\boldsymbol{e}}_z$, and the effective vector potential is given as $\boldsymbol{A}_n^E = \boldsymbol{A}^E = \frac{1}{c}\boldsymbol{E} \times \boldsymbol{e}_z$. The magnon Hamiltonian in the presence of an electric field is written as

$$\begin{aligned} H^J &= J_1 S \sum_{i,\delta} \left(a_{i,1} a_{i+\delta,2} e^{i\theta^N_{r_i,r_i+\delta}} + \text{H.c.}\right), \\ H^D &= -\sum_{i,\vartheta} iD_2 S \Big(a_{i,1}^\dagger a_{i+\vartheta,1} e^{-i\theta^{\text{NN}}_{r_i,r_i+\vartheta}} \\ &\quad - a_{i,2}^\dagger a_{i+\vartheta,2} e^{i\theta^{\text{NN}}_{r_i,r_i+\vartheta}} + \text{H.c.}\Big), \end{aligned} \quad \text{(B9)}$$

where the phase accumulated along the nearest-neighbor (second-nearest-neighbor) hopping is given as

$$\begin{aligned} \theta^N_{r_i,r_i+\delta} &= -\frac{g\mu_B}{\hbar c^2} \int_{r_i}^{r_i+\delta} [\boldsymbol{E}(t) \times \boldsymbol{e}_z] \cdot d\boldsymbol{r}, \\ \theta^{\text{NN}}_{r_i,r_i+\vartheta} &= -\frac{g\mu_B}{\hbar c^2} \int_{r_i}^{r_i+\vartheta} [\boldsymbol{E}(t) \times \boldsymbol{e}_z] \cdot d\boldsymbol{r}. \end{aligned} \quad \text{(B10)}$$

If the scale of the spatial variance of $\boldsymbol{E}$ is much larger than the lattice constant, one obtains

$$\begin{aligned} \theta^N_{r_i,r_i+\delta} &= \frac{g\mu_B}{\hbar c} \boldsymbol{A}^E \cdot \boldsymbol{\delta}, \\ \theta^{\text{NN}}_{r_i,r_i+\vartheta} &= \frac{g\mu_B}{\hbar c} \boldsymbol{A}^E \cdot \boldsymbol{\vartheta}. \end{aligned} \quad \text{(B11)}$$

Making use of the Fourier transformation Eq. (A9), one directly obtains $H = \sum_{\boldsymbol{k}} \Psi_{\boldsymbol{k}}^\dagger \mathcal{H}(\boldsymbol{k} - \frac{g\mu_B}{\hbar c}\boldsymbol{A}) \Psi_{\boldsymbol{k}}$, with the Nambu basis given by $\Psi_{\boldsymbol{k}}^\dagger = (a_{\boldsymbol{k},1}^\dagger, a_{\boldsymbol{k},2}^\dagger, a_{-\boldsymbol{k},1}, a_{-\boldsymbol{k},2})$, where $A_{mn}(\boldsymbol{k}) - C_{mn}$ is diagonal with $A_{11(22)}(\boldsymbol{k}) - C_{11(22)} = \frac{S}{2}[3J_1 - K(2S-1)/S \pm D\sum_\delta 2\sin(\boldsymbol{k}\cdot\boldsymbol{\delta})]$, and $B_{mn}(\boldsymbol{k})$ is nondiagonal with $B_{12}(\boldsymbol{k}) = B_{21}^*(\boldsymbol{k}) = \frac{S}{2}[\sum_{\boldsymbol{\vartheta}} \exp(i\boldsymbol{k}\cdot\boldsymbol{\vartheta})]$.

APPENDIX C: GAUGE TRANSFORMATION AND DIPOLE INTERACTION

In this Appendix, we present a gauge transformation to derive a perturbed Hamiltonian in the form of a dipole interaction. The single-particle Hamiltonian and the Bloch Hamiltonian satisfy

$$\mathcal{H}_0(-i\nabla, \boldsymbol{r}) = e^{i\boldsymbol{k}\cdot\boldsymbol{r}} \mathcal{H}_0(\boldsymbol{k}) e^{-i\boldsymbol{k}\cdot\boldsymbol{r}}. \quad \text{(C1)}$$

According to Sec. II, the perturbed Hamiltonian is written as

$$\mathcal{H}_A = \mathcal{H}_0\left(-i\nabla + \frac{g\mu_B}{\hbar c}\boldsymbol{A}, \boldsymbol{r}\right). \quad \text{(C2)}$$

The time-dependent Schrödinger equation is

$$i\hbar \frac{\partial |\psi(\boldsymbol{r},t)\rangle}{\partial t} = \mathcal{H}_A |\psi(\boldsymbol{r},t)\rangle. \quad \text{(C3)}$$

There is a freedom of choice regarding the phase of the wave functions. A unitary gauge transformation of $|\psi(\boldsymbol{r},t)\rangle$ takes the form

$$|\psi'(\boldsymbol{r},t)\rangle = \mathcal{U}(t) |\psi(\boldsymbol{r},t)\rangle. \quad \text{(C4)}$$

The time-dependent Schrödinger equation transforms as

$$i\hbar \frac{\partial |\psi'(\boldsymbol{r},t)\rangle}{\partial t} = \left[\mathcal{U}\mathcal{H}_A\mathcal{U}^\dagger |\psi(\boldsymbol{r},t)\rangle + i\hbar \frac{\partial \mathcal{U}(t)}{\partial t}\mathcal{U}^\dagger(t)\right] |\psi'(\boldsymbol{r},t)\rangle. \quad \text{(C5)}$$

The unitary transformation is chosen as $\mathcal{U}(t) = e^{i\mathcal{S}(t)}$, with

$$\mathcal{S}(t) = \frac{g\mu_B}{\hbar c}\boldsymbol{A}(t) \cdot \boldsymbol{r}. \quad \text{(C6)}$$

For the first term on the right-hand side of Eq. (C5), with use of the Baker-Campbell-Hausdorff identity

$$\begin{aligned} e^{i\mathcal{S}} \mathcal{H}_A e^{-i\mathcal{S}} &= \mathcal{H} + i[\mathcal{S}, \mathcal{H}_A] - \frac{1}{2}[\mathcal{S}, [\mathcal{S}, \mathcal{H}_A]] \cdots \\ &\quad + \frac{i^n}{n!}[\mathcal{S}, \ldots, [\mathcal{S}, \mathcal{H}_A]] + \cdots, \end{aligned} \quad \text{(C7)}$$

it is obtained that

$$\mathcal{U}(t)\mathcal{H}_A\mathcal{U}^\dagger(t) = \mathcal{H}_0. \quad \text{(C8)}$$

For the second term on the right-hand side of Eq. (C5), by introducing the effective electric field $\tilde{\boldsymbol{E}} = -\partial_t \boldsymbol{A}$, it is straightforward to show that

$$i\hbar \frac{\partial \mathcal{U}(t)}{\partial t}\mathcal{U}^\dagger(t) = \frac{g\mu_B}{c}\tilde{\boldsymbol{E}}(t) \cdot \boldsymbol{r}. \quad \text{(C9)}$$

Then the Hamiltonian in the velocity gauge transforms to

$$\mathcal{H}_E(t) = \mathcal{H}_0(\boldsymbol{k}) + \frac{g\mu_B}{c}\tilde{\boldsymbol{E}}(t)\cdot\boldsymbol{r}. \tag{C10}$$

APPENDIX D: MAGNON SPIN CURRENT

Now we define the magnon spin current. Because the z component of the total spin is conserved, the local magnon spin density (LMSD) is $n_z(\boldsymbol{r}_i) = \hbar\sum_m \boldsymbol{z}_m a^\dagger_{i,m}a_{i,m}$, satisfying the continuity equation. The Fourier transformation of the LMSD is written as

$$n_z(\boldsymbol{r}_i) = \frac{\hbar}{N}\sum_{\boldsymbol{k}\boldsymbol{q}m}\boldsymbol{z}_m e^{-i\boldsymbol{q}\cdot(\boldsymbol{r}_i+\boldsymbol{t}_m)}a^\dagger_{\boldsymbol{k}+\boldsymbol{q},m}a_{\boldsymbol{k},m}. \tag{D1}$$

The Heisenberg equation of motion for $a_{\boldsymbol{k},m}$ is used to derive the equation of motion for $n_z(\boldsymbol{r}_i)$:

$$\begin{aligned}\dot{a}_{\boldsymbol{k},m} =& \frac{1}{i\hbar}[a_{\boldsymbol{k},m}, H]\\ =& \frac{1}{i\hbar}\sum_n (A_{\boldsymbol{k},mn}a_{\boldsymbol{k},n} + A_{\boldsymbol{k},mn}a_{\boldsymbol{k},n} + B^*_{\boldsymbol{k},mn}a_{-\boldsymbol{k},n})\\ =& \frac{1}{i\hbar}\sum_n (2A_{\boldsymbol{k},mn}a_{\boldsymbol{k},n} + B_{\boldsymbol{k},mn}a^\dagger_{-\boldsymbol{k},n} + B_{-\boldsymbol{k},nm}a^\dagger_{-\boldsymbol{k},n}),\end{aligned} \tag{D2}$$

where H is given by Eq. (A10), and we obtain

$$\begin{aligned}\frac{\partial n_z(\boldsymbol{r}_i)}{\partial t} =& \frac{1}{iN}\sum_{\boldsymbol{k}\boldsymbol{q}mn} e^{-i\boldsymbol{q}\cdot\boldsymbol{r}_{i,m}}\boldsymbol{z}_m[-(2A_{\boldsymbol{k}+\boldsymbol{q},nm}a^\dagger_{\boldsymbol{k}+\boldsymbol{q},n}\\ &+ (B^*_{\boldsymbol{k}+\boldsymbol{q},mn} + B^*_{-\boldsymbol{k}-\boldsymbol{q},nm})a^\dagger_{-\boldsymbol{k}-\boldsymbol{q},n})a_{\boldsymbol{k},m}\\ &+ a^\dagger_{\boldsymbol{k}+\boldsymbol{q},m}(2A_{\boldsymbol{k},mn}a_{\boldsymbol{k},n} + (B_{\boldsymbol{k},mn} + B_{-\boldsymbol{k},nm})a^\dagger_{-\boldsymbol{k},n})].\end{aligned} \tag{D3}$$

In the case of $\sum\boldsymbol{\delta} = \boldsymbol{0}$, and assuming the long-wavelength limit $\boldsymbol{q}\to\boldsymbol{0}$, the magnon spin current is obtained with use of the continuity equation $\partial n_{z\boldsymbol{q}}/\partial t + i\boldsymbol{q}\cdot\boldsymbol{J}_{s,z} = \boldsymbol{0}$, which is given as

$$\begin{aligned}\boldsymbol{J}_{s,z} =& \hbar\sum_{kmn}\boldsymbol{z}_m\left(\frac{\partial A_{\boldsymbol{k},mn}}{\partial\boldsymbol{k}}a^\dagger_{\boldsymbol{k},m}a_{\boldsymbol{k},n} + \frac{\partial A_{-\boldsymbol{k},nm}}{\partial\boldsymbol{k}}a_{-\boldsymbol{k},m}a^\dagger_{-\boldsymbol{k},n}\right.\\ &\left. + \frac{\partial B_{\boldsymbol{k},mn}}{\partial\boldsymbol{k}}a^\dagger_{\boldsymbol{k},m}a^\dagger_{-\boldsymbol{k},n} + \frac{\partial B^*_{\boldsymbol{k},nm}}{\partial\boldsymbol{k}}a_{-\boldsymbol{k},m}a_{\boldsymbol{k},n}\right)\\ =& \hbar\sum_{\boldsymbol{k}}\Psi^\dagger_{\boldsymbol{k}}\mathcal{Z}\frac{\partial\mathcal{H}_{\boldsymbol{k}}}{\partial\boldsymbol{k}}\Psi_{\boldsymbol{k}}.\end{aligned} \tag{D4}$$

When the long-wavelength limit is invoked, the continuous translational symmetry is respected by removing the dependences on the lattice structure's long-wavelength limit. In the low temperature we considered, the spin-wave excitation is dominated by the long-wave modes, which justifies the use of the long-wave approximation. In Eq. (D4) we define the diagonal matrix $\mathcal{Z}$,

$$\mathcal{Z} = \mathrm{diag}(z_1,\ldots,z_N,z_1,\ldots,z_N). \tag{D5}$$

Making use of Eq. (10), we have

$$\boldsymbol{J}_{s,z} = \hbar\sum_{\boldsymbol{k}}\Phi^\dagger_{\boldsymbol{k}}\Sigma_z\frac{\widetilde{\partial\mathcal{Z}\mathcal{H}_{\boldsymbol{k}}}}{\partial\boldsymbol{k}}\Phi_{\boldsymbol{k}}. \tag{D6}$$

It is found that

$$\frac{\widetilde{\partial\mathcal{Z}\mathcal{H}_{\boldsymbol{k}}}}{\partial\boldsymbol{k}} = \frac{\partial\widetilde{\mathcal{Z}\mathcal{H}}_{\boldsymbol{k}}}{\partial\boldsymbol{k}} - \widetilde{\mathcal{Z}\mathcal{H}}_{\boldsymbol{k}}U_{\boldsymbol{k}}^{-1}\frac{\partial U_{\boldsymbol{k}}}{\partial\boldsymbol{k}} - \frac{\partial U_{\boldsymbol{k}}^{-1}}{\partial\boldsymbol{k}}U_{\boldsymbol{k}}\widetilde{\mathcal{Z}\mathcal{H}}_{\boldsymbol{k}}, \tag{D7}$$

and we obtain

$$\boldsymbol{J}_{s,z} = \hbar\sum_{\boldsymbol{k}}\Phi^\dagger_{\boldsymbol{k}}\Sigma_z\left(\frac{\partial\widetilde{\mathcal{Z}\mathcal{H}}_{\boldsymbol{k}}}{\partial\boldsymbol{k}} - i[\boldsymbol{\mathcal{A}}_{\boldsymbol{k}},\widetilde{\mathcal{Z}\mathcal{H}}_{\boldsymbol{k}}]\right)\Phi_{\boldsymbol{k}}, \tag{D8}$$

where the Berry connection is defined by

$$\boldsymbol{\mathcal{A}}_{\boldsymbol{k}} = iU_{\boldsymbol{k}}^{-1}\frac{\partial U_{\boldsymbol{k}}}{\partial\boldsymbol{k}} = i\Sigma_z U_{\boldsymbol{k}}^\dagger\Sigma_z\frac{\partial U_{\boldsymbol{k}}}{\partial\boldsymbol{k}}. \tag{D9}$$

Note that the Berry connection given in Eq. (D9) is different from $iU_{\boldsymbol{k}}^\dagger\frac{\partial U_{\boldsymbol{k}}}{\partial\boldsymbol{k}}$. This is because the Bogoliubov transformation is generally not unitary [64].

For collinear ferromagnets, due to the reduction of the $2N$-dimensional basis to the N-dimensional basis $\Psi^\dagger_{\boldsymbol{k}} = (a^\dagger_{\boldsymbol{k},1},\ldots,a^\dagger_{\boldsymbol{k},N})$, the direction matrix $\mathcal{Z}$ in Eq. (D5) becomes a unit matrix, and the magnon spin-current operator in Eq. (D8) becomes

$$\boldsymbol{J}_s = \hbar\sum_{\boldsymbol{k}}\Phi^\dagger_{\boldsymbol{k}}\left(\frac{\partial\mathcal{H}_{\boldsymbol{k}}}{\partial\boldsymbol{k}} - i[\boldsymbol{\mathcal{A}}_{\boldsymbol{k}},\mathcal{H}_{\boldsymbol{k}}]\right)\Phi_{\boldsymbol{k}}. \tag{D10}$$

APPENDIX E: MAGNON SPIN PHOTOCURRENT IN COLLINEAR FERROMAGNETS

In this Appendix, we derive the equations of motion for the magnon density matrix in the presence of the AC phase induced by the electric field of light. A similar method for electron second-order optical responses is used to calculate the electric bulk photogalvanic effect [37,65]. We give the formalism of nonlinear responses for the magnon spin photocurrent using the standard perturbation technique. According to Eq. (7) in the main text, the recursion equation can be rewritten as

$$\begin{aligned}\rho^{(n+1)}_{mn}(\omega) =& \frac{g\mu_B}{\hbar c^2}d_{mn}(\omega)\\ &\times\int\frac{d\omega_1}{2\pi}\omega_1\epsilon^{\alpha_1 z\beta}E^{\alpha_1}D^\beta[\rho^{(n)}(\omega-\omega_1)]_{mn},\end{aligned} \tag{E1}$$

where $\epsilon^{\alpha_1 z\beta}$ is the Levi-Civita symbol, and summation is implied over repeated spatial indices. In deriving the second-order reduced density matrix, it can be divided into terms originating from the intraband (i) and interband (e) components of the $\mathcal{D}_{\mathrm{opt}}$ operator:

$$\begin{aligned}\rho^{(2)}_{mn}(\omega) =& \nu_c\sum_X\int\frac{d\omega_1 d\omega_2}{(2\pi)^2}\omega_1\omega_2E^{\alpha_1}(\omega_1)\\ &\times E^{\alpha_2}(\omega_2)\epsilon^{\alpha_1 z\beta}\epsilon^{\alpha_2 z\gamma}\varrho^{X,\beta\gamma}_{mn}(\omega_1,\omega_2),\end{aligned} \tag{E2}$$

where the constant $\frac{g^2\mu_B^2}{\hbar^2c^4}$ is denoted as ν_c. Then, the contribution of each term in Eq. (E2) to the spin photoconductivities is denoted as $\sigma_X^{\alpha\alpha_1\alpha_2}$ for $X =$ ii, ie, ei, and ee. Keeping in mind

that the energy conservation $\omega = \omega_1 + \omega_2$ is always satisfied, the expressions for each term are obtained as

$$\begin{aligned}
\varrho^{\mathrm{ii},\beta\gamma}_{mn}(\omega_1,\omega_2) &= -\,d_{mn}(\omega)d_{mn}(\omega_2)(\partial^\beta\partial^\gamma g_m)\delta_{mn},\\
\varrho^{\mathrm{ei},\beta\gamma}_{mn}(\omega_1,\omega_2) &= -\,id_{mn}(\omega)d_{mm}(\omega_2)\mathcal{A}^\gamma_{mn}\partial^\beta g_{nm},\\
\varrho^{\mathrm{ie},\beta\gamma}_{mn}(\omega_1,\omega_2) &= -\,id_{mn}(\omega)\big(\partial^\gamma\big[d_{mn}(\omega_2)\mathcal{A}^\beta_{mn}g_{nm}\big] - i\big(\mathcal{A}^\gamma_{mm}-\mathcal{A}^\gamma_{nn}\big)\big[d_{mn}(\omega_2)\mathcal{A}^\beta_{mn}g_{nm}\big]\big),\\
\varrho^{\mathrm{ee},\beta\gamma}_{mn}(\omega_1,\omega_2) &= \sum_{p\neq m,n} d_{mn}(\omega)\big[\mathcal{A}^\gamma_{mp}d_{pn}(\omega_2)\mathcal{A}^\beta_{pn}g_{np} - \mathcal{A}^\gamma_{pn}d_{mp}(\omega_2)\mathcal{A}^\beta_{mp}g_{pm}\big],
\end{aligned} \tag{E3}$$

where we define $g_{mn} = g_m - g_n$. Note that ϱ^{ii} and ϱ^{ei} include the derivative to the Bose-Einstein distribution. Together with Eqs. (D8) and (E3), the second-order magnon spin current is given as

$$J^{(2),\alpha}_s(\omega_1,\omega_2) = \sum_X E^\beta(\omega_1)E^\gamma(\omega_2)\chi_X^{\alpha\beta\gamma}(\omega_1,\omega_2), \tag{E4}$$

with

$$\chi_{\mathrm{ii}}^{\alpha\alpha_1\alpha_2} = -\frac{\nu_c}{2}\int[d\boldsymbol{k}]\sum_m \epsilon^{\alpha_1 z\beta}\epsilon^{\alpha_2 z\gamma}\omega_1\omega_2 J^\alpha_{s,mm}d_{mm}(\omega_2)d_{mm}(\omega)\partial^\beta\partial^\gamma g_m \tag{E5}$$

$$+[(\alpha_1,\omega_1)\leftrightarrow(\alpha_2,\omega_2)], \tag{E6}$$

$$\chi_{\mathrm{ei}}^{\alpha\alpha_1\alpha_2} = -\frac{\nu_c}{2}\int[d\boldsymbol{k}]\sum_{m,n} i\epsilon^{\alpha_1 z\beta}\epsilon^{\alpha_2 z\gamma}\omega_1\omega_2 J^\alpha_{s,mn}d_{nm}(\omega)d_{mm}(\omega_2)\mathcal{A}^\gamma_{nm}\partial^\beta g_{nm} \tag{E7}$$

$$+[(\alpha_1,\omega_1)\leftrightarrow(\alpha_2,\omega_2)], \tag{E8}$$

$$\chi_{\mathrm{ie}}^{\alpha\alpha_1\alpha_2} = -\frac{\nu_c}{2}\int[d\boldsymbol{k}]\sum_{m,n} i\epsilon^{\alpha_1 z\beta}\epsilon^{\alpha_2 z\gamma}\omega_1\omega_2 J^\alpha_{s,mn}d_{nm}(\omega)\big(\partial^\beta\big[d_{nm}(\omega_2)\mathcal{A}^\gamma_{nm}g_{nm}\big] - i\big(\mathcal{A}^\beta_{nn}-\mathcal{A}^\beta_{mm}\big)$$

$$\times\big[d_{nm}(\omega_2)\mathcal{A}^\gamma_{nm}g_{nm}\big]\big) + [(\alpha_1,\omega_1)\leftrightarrow(\alpha_2,\omega_2)], \tag{E9}$$

$$\chi_{\mathrm{ee}}^{\alpha\alpha_1\alpha_2} = \frac{\nu_c}{2}\int[d\boldsymbol{k}]\sum_{m,n,p}\epsilon^{\alpha_1 z\beta}\epsilon^{\alpha_2 z\gamma}\omega_1\omega_2 J^\alpha_{s,mn}d_{nm}(\omega)\big[d_{pm}(\omega_2)\mathcal{A}^\beta_{np}\mathcal{A}^\gamma_{pm}g_{mp} - d_{np}(\omega_2)\mathcal{A}^\beta_{pm}\mathcal{A}^\gamma_{np}g_{pn}\big] + [(\alpha_1,\omega_1)\leftrightarrow(\alpha_2,\omega_2)]. \tag{E10}$$

Note that the conductivity tensors are symmetrized by the indices and frequencies of electric fields. This is because the physical observables should not be affected by an arbitrary permutation of applied external fields, that is, the conductivity tensor has intrinsic permutation symmetry [37,66]. It is clearly seen that the magnon photocurrent is quite different from the case of charge photocurrent. For the magnon photocurrent, the electric field is restricted to the plane perpendicular to the axis of the magnon spin, while for the charge case the direction of the electric field can be arbitrary.

1. Drude spin current

According to Eq. (E6), $\chi_{\mathrm{ii}}^{\alpha\alpha_1\alpha_2}$ only involves the intraband contribution, which is given by

$$\chi_{\mathrm{ii}}^{\alpha\alpha_1\alpha_2} = -\lim_{\omega\to 0}\frac{\nu_c}{2\hbar^2\omega}\int[d\boldsymbol{k}]\sum_m\left(\epsilon^{\alpha_1 z\beta}\epsilon^{\alpha_2 z\gamma}\frac{1}{-\Omega} + \epsilon^{\alpha_2 z\beta}\epsilon^{\alpha_1 z\gamma}\frac{1}{\omega+\Omega}\right)\Omega(\omega+\Omega)J^\alpha_{s,mm}\partial^\beta\partial^\gamma g_m. \tag{E11}$$

It describes the drift movement of magnons driven by the optical field, and it is called the Drude contribution. Following the definitions

$$\begin{aligned}
\eta^{\alpha\alpha_1\alpha_2} &= \tfrac{1}{2}\mathrm{Re}(\chi^{\alpha\alpha_1\alpha_2} + \chi^{\alpha\alpha_2\alpha_1}),\\
\kappa^{\alpha\alpha_1\alpha_2} &= \tfrac{1}{2}\mathrm{Im}(\chi^{\alpha\alpha_1\alpha_2} - \chi^{\alpha\alpha_2\alpha_1}),
\end{aligned} \tag{E12}$$

we obtain the LP spin photocurrent conductivity

$$\eta_{\mathrm{D}}^{\alpha\alpha_1\alpha_2} = \frac{\nu_c}{2\hbar^2}\int[d\boldsymbol{k}]\sum_m(\epsilon^{\alpha_1 z\beta}\epsilon^{\alpha_2 z\gamma} + \epsilon^{\alpha_2 z\beta}\epsilon^{\alpha_1 z\gamma})v^\alpha_m\partial^\beta\partial^\gamma g_m. \tag{E13}$$

In Eq. (E11) we use the relation $J^\alpha_{s,mm} = \hbar v_m$, with $v_m = \frac{1}{\hbar}\partial^\alpha\varepsilon_m$ being the group velocity. To simplify the formulas, we define the symmetric combination of the Levi-Civita symbols as

$$E_S^{\alpha_1\alpha_2\beta\gamma} = \epsilon^{\alpha_1 z\beta}\epsilon^{\alpha_2 z\gamma} + \epsilon^{\alpha_2 z\beta}\epsilon^{\alpha_1 z\gamma} \tag{E14}$$

and the antisymmetric combination as

$$E_A^{\alpha_1\alpha_2\beta\gamma} = \epsilon^{\alpha_1 z\beta}\epsilon^{\alpha_2 z\gamma} - \epsilon^{\alpha_2 z\beta}\epsilon^{\alpha_1 z\gamma}, \tag{E15}$$

and we have

$$\eta_{\rm D}^{\alpha\alpha_1\alpha_2} = \frac{\nu_c}{2\hbar}\int [d\boldsymbol{k}] \sum_m E_S^{\alpha_1\alpha_2\beta\gamma} v_m^\alpha \partial^\beta \partial^\gamma g_m. \tag{E16}$$

Note that the integrand $v_m^\alpha \partial^\beta \partial^\gamma g_m$ in Eq. (E16) is symmetric by exchanging the external field indices β and γ, hence $E_S^{\alpha_1\alpha_2\beta\gamma} = 2$ for $\alpha_1 = \alpha_2$ while $E_S^{\alpha_1\alpha_2\beta\gamma} = -2$ for $\alpha_1 \neq \alpha_2$, and Eq. (E16) can be rewritten as

$$\eta_{\rm D}^{\alpha\alpha_1\alpha_2} = \varsigma\frac{\nu_c}{\hbar}\int [d\boldsymbol{k}] \sum_m v_m^\alpha \partial^{\alpha_1} \partial^{\alpha_2} g_m, \tag{E17}$$

where we define $\varsigma = 1$ for $\alpha_1 = \alpha_2$ and $\varsigma = -1$ for $\alpha_1 \neq \alpha_2$. Note that for the LP Drude response, it is independent of the frequency of the light.

The CP-component is given as

$$\begin{aligned}\kappa_{\rm ii}^{\alpha\alpha_1\alpha_2} &= -\lim_{\omega\to 0}\frac{i\nu_c}{2\hbar\omega}\int [d\boldsymbol{k}] \sum_m E_S^{\alpha_1\alpha_2\beta\gamma}\left(\frac{1}{-\Omega} - \frac{1}{\omega+\Omega}\right)\Omega(\omega+\Omega) v_m^\alpha \partial^\beta \partial^\gamma g_m \\ &= -\lim_{\omega\to 0}\frac{i\nu_c}{\hbar\omega}\int [d\boldsymbol{k}] \sum_m E_S^{\alpha_1\alpha_2\beta\gamma}\Omega v_m^\alpha \partial^\beta \partial^\gamma g_m.\end{aligned} \tag{E18}$$

For the CP responses, the external field indices are restricted by $\alpha_1 \neq \alpha_2$. Making use of the exchanging symmetric property of the integrand $v_m^\alpha \partial^\beta \partial^\gamma g_m$, it is easy to verify that the CP-response vanishes.

2. Berry curvature dipole spin current

In this subsection, we consider the spin photocurrent originating from $\chi_{s,\rm ei}^{\alpha\alpha_1\alpha_2}$. For the dc current, it is given as

$$\chi_{\rm ei}^{\alpha\alpha_1\alpha_2} = \lim_{\omega\to 0}\frac{\nu_c}{2\hbar}\int [d\boldsymbol{k}] \sum_{m\neq n}\left(\epsilon^{\alpha_1 z\beta}\epsilon^{\alpha_2 z\gamma}\frac{1}{-\Omega} + \epsilon^{\alpha_2 z\beta}\epsilon^{\alpha_1 z\gamma}\frac{1}{\omega+\Omega}\right)\Omega(\omega+\Omega)\mathcal{A}_{mn}^\alpha \mathcal{A}_{nm}^\gamma \partial^\beta g_{nm}, \tag{E19}$$

where we used the relation $\lim_{\omega\to 0} d_{nm}(\omega) J_{s,mn}^\mu = i\hbar^{-1}\mathcal{A}_{mn}^\mu$ for $m \neq n$. The LP-photocurrent tensor is

$$\begin{aligned}\eta_{\rm ei}^{\alpha\alpha_1\alpha_2} &= \lim_{\omega\to 0}\frac{\nu_c\omega}{2\hbar}\int [d\boldsymbol{k}] \sum_{m\neq n}\left(\epsilon^{\alpha_1 z\beta}\epsilon^{\alpha_2 z\gamma} + \epsilon^{\alpha_2 z\beta}\epsilon^{\alpha_1 z\gamma}\right)\mathcal{A}_{mn}^\alpha \mathcal{A}_{nm}^\gamma \partial^\beta g_{nm} \\ &= \lim_{\omega\to 0}\frac{\nu_c\omega}{2\hbar}\int [d\boldsymbol{k}] \sum_{m\neq n} E_S^{\alpha_1\alpha_2\beta\gamma}\left(\mathcal{A}_{mn}^\alpha \mathcal{A}_{nm}^\gamma - \mathcal{A}_{mn}^\gamma \mathcal{A}_{nm}^\alpha\right)\partial^\beta g_m.\end{aligned} \tag{E20}$$

It can be seen that the LP response vanishes for the dc current. The CP-photocurrent tensor is derived as

$$\kappa_{\rm BCD}^{\alpha\alpha_1\alpha_2} = i\frac{\nu_c\Omega}{2\hbar}\int [d\boldsymbol{k}] \sum_{m\neq n}(\epsilon^{\alpha_1 z\beta}\epsilon^{\alpha_2 z\gamma} - \epsilon^{\alpha_2 z\beta}\epsilon^{\alpha_1 z\gamma})\mathcal{A}_{mn}^\alpha \mathcal{A}_{nm}^\gamma \partial^\beta g_{nm} = \frac{\nu_c\Omega}{2\hbar^2}\int [d\boldsymbol{k}] \sum_m E_A^{\alpha_1\alpha_2\beta\gamma} i\epsilon^{\alpha\gamma\tau}\partial^\beta \Omega_m^\tau g_m. \tag{E21}$$

The magnon Berry curvature is defined as

$$\Omega_m^\tau = \frac{i}{2}\epsilon^{\alpha\gamma\tau}\sum_{n\neq m}\left(\mathcal{A}_{mn}^\alpha \mathcal{A}_{nm}^\gamma - \mathcal{A}_{m,n}^\gamma \mathcal{A}_{nm}^\alpha\right). \tag{E22}$$

With use of Eq. (E22) and partial integration, Eq. (E21) can be rewritten depending on the frequency of incident light as $O(\Omega)$,

$$\kappa_{\rm BCD}^{\alpha\alpha_1\alpha_2} = \frac{\nu_c\Omega}{2\hbar}\int [d\boldsymbol{k}] \sum_m E_A^{\alpha_1\alpha_2\beta\gamma}\epsilon^{\alpha\gamma\tau}\partial^\beta \Omega_m^\tau g_m = \frac{\nu_c\Omega}{2\hbar}\int [d\boldsymbol{k}] \sum_m \left(\epsilon^{\alpha\alpha_2\tau}\partial^{\alpha_1} - \epsilon^{\alpha\alpha_1\tau}\partial^{\alpha_2}\right)\Omega_m^\tau g_m. \tag{E23}$$

It is clear that this comes from the dipole of Berry curvature in momentum space. The BCD contribution is classified as a CP photocurrent. The BCD-induced nonlinear current has been extensively studied in electric systems. In bosonic systems, the magnon BSC driven by temperature gradient has been proposed [35]. Here we reveal the BCD contribution to magnon spin current generated via the light method.

3. Injection and rectification spin currents

Now we study the spin photocurrent coming from $\chi_{\rm ee}$. First we consider the contribution from the diagonal component of $\chi_{\rm ee}$ with $m = n$, denoted as $\chi_{\rm ee,d}$, which is given by

$$\begin{aligned}\chi^{\alpha\alpha_1\alpha_2}_{\rm ee,d} &= \lim_{\omega\to 0}\frac{\nu_c\hbar}{2\omega}\int[d\boldsymbol{k}]\sum_{m\neq p}\epsilon^{\alpha_1 z\beta}\epsilon^{\alpha_2 z\gamma}\omega_1\omega_2\Delta^{\alpha}_{mp}d_{pm}(\omega_2)\mathcal{A}^{\beta}_{mp}\mathcal{A}^{\gamma}_{pm}g_{mp} + [(\alpha_1,\omega_1)\leftrightarrow(\alpha_2,\omega_2)]\\ &= \lim_{\omega\to 0}\frac{\nu_c\hbar}{2\hbar\omega}\int[d\boldsymbol{k}]\sum_{m\neq p}\left(\epsilon^{\alpha_1 z\beta}\epsilon^{\alpha_2 z\gamma}\frac{1}{-\hbar\Omega-\varepsilon_{pm}} + \epsilon^{\alpha_2 z\beta}\epsilon^{\alpha_1 z\gamma}\frac{1}{\hbar\omega+\hbar\Omega-\varepsilon_{pm}}\right)\Omega(\omega+\Omega)\Delta^{\alpha}_{mp}\mathcal{A}^{\beta}_{mp}\mathcal{A}^{\gamma}_{pm}g_{mp},\end{aligned}\tag{E24}$$

where Δ^{α}_{mp} is the interband-transition of the velocity. Making use of Eqs. (E14) and (E15), we have

$$\begin{aligned}\eta^{\alpha\alpha_1\alpha_2}_{\rm ee,d} &= \lim_{\omega\to 0}\frac{\nu_c\hbar}{2\omega}\int[d\boldsymbol{k}]\sum_{m\neq p}E_S^{\alpha_1\alpha_2\beta\gamma}\left(\frac{1}{-\hbar\Omega-\varepsilon_{pm}}+\frac{1}{\hbar\omega+\hbar\Omega-\varepsilon_{pm}}\right)\Omega(\omega+\Omega)\Delta^{\alpha}_{mp}\mathcal{A}^{\beta}_{mp}\mathcal{A}^{\gamma}_{pm}g_{mp}\\ &= \lim_{\omega\to 0}\frac{\nu_c\hbar}{2\omega}\int[d\boldsymbol{k}]\sum_{m\neq p}E_S^{\alpha_1\alpha_2\beta\gamma}\left(\frac{1}{-\hbar\Omega-\varepsilon_{pm}}\mathcal{A}^{\beta}_{mp}\mathcal{A}^{\gamma}_{pm}+\frac{1}{\hbar\omega+\hbar\Omega+\varepsilon_{pm}}\mathcal{A}^{\beta}_{pm}\mathcal{A}^{\gamma}_{mp}\right)\Omega(\omega+\Omega)\Delta^{\alpha}_{mp}g_{mp}\,.\end{aligned}\tag{E25}$$

Because of the prefactor $1/\omega$, Eq. (E25) diverges with the limit $\omega\to 0$. Therefore, $O(\omega)$ and $O(\omega^0)$ are retained. Performing the Taylor expansion,

$$\frac{1}{\hbar\omega+\Omega+\varepsilon_{nm}} = \frac{1}{\hbar\Omega+\varepsilon_{nm}} - \frac{\omega}{(\hbar\Omega+\varepsilon_{nm})^2} + O(\omega^2),\tag{E26}$$

and with use of the Cauchy principal integral,

$$\frac{1}{\hbar\Omega+i0^+\varepsilon_{nm}} = \mathrm{P}(\frac{1}{\hbar\Omega-\varepsilon_{mn}}) - i\pi\delta(\hbar\Omega-\varepsilon_{mn}),\tag{E27}$$

where P denotes the principal value. We have

$$\begin{aligned}\eta^{\alpha\alpha_1\alpha_2}_{\rm ee,d} &= -\lim_{\omega\to 0}\frac{i\pi\nu_c\hbar}{2\omega}\int[d\boldsymbol{k}]\sum_{m\neq n}E_S^{\alpha_1\alpha_2\beta\gamma}\delta(\hbar\Omega-\varepsilon_{mn})\Omega(\omega+\Omega)\Delta^{\alpha}_{mn}\left(\mathcal{A}^{\beta}_{mn}\mathcal{A}^{\gamma}_{nm}+\mathcal{A}^{\beta}_{nm}\mathcal{A}^{\gamma}_{mn}\right)g_{mn}\\ &\quad -\lim_{\omega\to 0}\frac{\nu_c\hbar}{2\omega}\int[d\boldsymbol{k}]\sum_{m\neq n}E_S^{\alpha_1\alpha_2\beta\gamma}\frac{\omega}{(\hbar\Omega-\varepsilon_{mn})^2}\Omega(\omega+\Omega)\Delta^{\alpha}_{mn}\mathcal{A}^{\beta}_{nm}\mathcal{A}^{\gamma}_{mn}g_{mn}.\end{aligned}\tag{E28}$$

Define the quantum metric and the Berry curvature,

$$G^{\beta\gamma}_{mn} = \tfrac{1}{2}\left(\mathcal{A}^{\beta}_{mn}\mathcal{A}^{\gamma}_{nm}+\mathcal{A}^{\gamma}_{mn}\mathcal{A}^{\beta}_{nm}\right),\tag{E29}$$

$$\Omega^{\beta\gamma}_{mn} = i\left(\mathcal{A}^{\beta}_{mn}\mathcal{A}^{\gamma}_{nm}-\mathcal{A}^{\gamma}_{mn}\mathcal{A}^{\beta}_{nm}\right).\tag{E30}$$

The first term in Eq. (E28) diverges as $\omega\to 0$, which is recognized as the injection current. Considering that the band-resolved quantum metric is symmetric with the indices permutation $\beta\leftrightarrow\gamma$, the injection current is

$$\begin{aligned}\eta^{\alpha\alpha_1\alpha_2}_{\rm Inj} &= -\lim_{\omega\to 0}\frac{i\pi\nu_c\hbar}{\omega}\int[d\boldsymbol{k}]\sum_{m\neq n}E_S^{\alpha_1\alpha_2\beta\gamma}\delta(\hbar\Omega-\varepsilon_{mn})\Omega^2\Delta^{\alpha}_{mn}G^{\beta\gamma}_{mn}g_{mn}\\ &= -\lim_{\omega\to 0}\varsigma\frac{i2\pi\nu_c}{\omega}\int[d\boldsymbol{k}]\sum_{m\neq n}\delta(\hbar\Omega-\varepsilon_{mn})\Omega^2\Delta^{\alpha}_{mn}G^{\alpha_1\alpha_2}_{mn}g_{mn}.\end{aligned}\tag{E31}$$

Note that the LP injection current diverges in the dc limit. This seemingly unphysical behavior can be eliminated by introducing the phenomenological scattering rate Γ, and the calculations are carried out by shifting the poles, i.e., the matrix $d_{mn}(\omega)$ is modified as

$$d_{mn}(\omega) = \frac{1}{\hbar\omega-\varepsilon_{mn}+i\varsigma}.\tag{E32}$$

In Eq. (E32) the relaxation-time approximation is invoked with $\varsigma = \alpha\omega = 1/\tau$, α is the Gilbert damping constant, and τ is the relaxation time. The δ function holds the property

$$\delta(\hbar\Omega-\varepsilon_{mn}) = \lim_{\varsigma\to 0}\frac{1}{\pi}\frac{\varsigma}{(\hbar\Omega-\varepsilon_{mn})^2+\varsigma^2}.\tag{E33}$$

With use of Eq. (E33), the injection current is given by

$$\eta_{\mathrm{Inj}}^{\alpha\alpha_1\alpha_2} = -\varsigma 2\nu_c\hbar\int[d\boldsymbol{k}]\sum_{m\neq n}\frac{\Omega^2}{(\hbar\Omega-\varepsilon_{mn})^2+\varsigma^2}\Delta_{mn}^{\alpha}G_{mn}^{\alpha_1\alpha_2}g_{mn}, \tag{E34}$$

hence it converges in the dc limit. The second term in Eq. (E28) is

$$\begin{aligned}\eta_{\mathrm{ee,d},2}^{\alpha\alpha_1\alpha_2} &= -\frac{\nu_c\hbar}{2}\int[d\boldsymbol{k}]\sum_{m\neq n}E_S^{\alpha_1\alpha_2\beta\gamma}\frac{1}{(\hbar\Omega-\varepsilon_{mn})^2}\Omega^2\Delta_{mn}^{\alpha}\mathcal{A}_{nm}^{\beta}\mathcal{A}_{mn}^{\gamma}g_{mn}\\ &= -2\varsigma\nu_c\hbar\int[d\boldsymbol{k}]\sum_{m\neq n}\frac{1}{(\hbar\Omega-\varepsilon_{mn})^2}\Omega^2\Delta_{mn}^{\alpha}G_{mn}^{\alpha_1\alpha_2}g_{mn}\\ &= -2\varsigma\nu_c\hbar\int[d\boldsymbol{k}]\sum_{m\neq n}\partial^{\alpha}\left(\frac{1}{\hbar\Omega-\varepsilon_{mn}}\right)\Omega^2G_{mn}^{\alpha_1\alpha_2}g_{mn}.\end{aligned} \tag{E35}$$

We will show in the following that Eq. (E35) is a part of the LP rectification current. The CP response of $\chi_{\mathrm{ee,d}}^{\alpha\alpha_1\alpha_2}$ is

$$\begin{aligned}\kappa_{\mathrm{ee,d}}^{\alpha\alpha_1\alpha_2} &= \lim_{\omega\to0}\frac{i\nu_c\hbar}{2\omega}\int[d\boldsymbol{k}]\sum_{m\neq n}E_A^{\alpha_1\alpha_2\beta\gamma}\left(\frac{1}{-\hbar\Omega-\varepsilon_{nm}}-\frac{1}{\hbar\omega+\hbar\Omega-\varepsilon_{nm}}\right)\Omega(\omega+\Omega)\Delta_{mn}^{\alpha}\mathcal{A}_{mn}^{\beta}\mathcal{A}_{nm}^{\gamma}g_{mn}\\ &= \lim_{\omega\to0}\frac{i\nu_c\hbar}{2\omega}\int[d\boldsymbol{k}]\sum_{m\neq n}E_A^{\alpha_1\alpha_2\beta\gamma}\left(\frac{1}{-\hbar\Omega-\varepsilon_{nm}}\mathcal{A}_{mn}^{\beta}\mathcal{A}_{nm}^{\gamma}-\frac{1}{\hbar\omega+\hbar\Omega+\varepsilon_{nm}}\mathcal{A}_{nm}^{\beta}\mathcal{A}_{mn}^{\gamma}\right)\Omega(\omega+\Omega)\Delta_{mn}^{\alpha}g_{mn}.\end{aligned} \tag{E36}$$

With use of Eqs. (E26) and (E27), we have

$$\begin{aligned}\kappa_{\mathrm{ee,d}}^{\alpha\alpha_1\alpha_2} &= \lim_{\omega\to0}\frac{\pi\nu_c\hbar}{2\omega}\int[d\boldsymbol{k}]\sum_{m\neq n}E_A^{\alpha_1\alpha_2\beta\gamma}\delta(\hbar\Omega-\varepsilon_{mn})\Omega(\omega+\Omega)\Delta_{mn}^{\alpha}\left(\mathcal{A}_{mn}^{\beta}\mathcal{A}_{nm}^{\gamma}-\mathcal{A}_{nm}^{\beta}\mathcal{A}_{mn}^{\gamma}\right)g_{mn}\\ &\quad-\lim_{\omega\to0}\frac{i\nu_c\hbar}{2\omega}\int[d\boldsymbol{k}]\sum_{m\neq n}E_A^{\alpha_1\alpha_2\beta\gamma}\mathrm{P}\frac{1}{\hbar\Omega-\varepsilon_{mn}}\Omega(\omega+\Omega)\Delta_{mn}^{\alpha}\left(\mathcal{A}_{mn}^{\beta}\mathcal{A}_{nm}^{\gamma}+\mathcal{A}_{nm}^{\beta}\mathcal{A}_{mn}^{\gamma}\right)g_{mn}\\ &\quad+\lim_{\omega\to0}\frac{i\nu_c\hbar}{2\omega}\int[d\boldsymbol{k}]\sum_{m\neq n}E_A^{\alpha_1\alpha_2\beta\gamma}\frac{\omega}{(\hbar\Omega-\varepsilon_{mn})^2}\Omega(\omega+\Omega)\Delta_{mn}^{\alpha}\mathcal{A}_{mn}^{\beta}\mathcal{A}_{nm}^{\gamma}g_{mn}.\end{aligned} \tag{E37}$$

The first term in Eq. (E37) is the CP injection current, which is written as

$$\begin{aligned}\kappa_{\mathrm{Inj}}^{\alpha\alpha_1\alpha_2} &= \lim_{\omega\to0}\frac{\pi\nu_c\hbar}{2\omega}\int[d\boldsymbol{k}]\sum_{m\neq n}E_A^{\alpha_1\alpha_2\beta\gamma}\delta(\hbar\Omega-\varepsilon_{mn})\Omega(\omega+\Omega)\Delta_{mn}^{\alpha}\left(\mathcal{A}_{mn}^{\beta}\mathcal{A}_{nm}^{\gamma}-\mathcal{A}_{nm}^{\beta}\mathcal{A}_{mn}^{\gamma}\right)g_{mn}\\ &= -\lim_{\omega\to0}\frac{i\pi\nu_c\hbar}{2\omega}\int[d\boldsymbol{k}]\sum_{m\neq n}E_A^{\alpha_1\alpha_2\beta\gamma}\delta(\hbar\Omega-\varepsilon_{mn})\Omega(\omega+\Omega)\Delta_{mn}^{\alpha}\Omega_{mn}^{\beta\gamma}g_{mn}\\ &= -\frac{\pi\nu_c\hbar}{2}\int[d\boldsymbol{k}]\sum_{m\neq n}E_A^{\alpha_1\alpha_2\beta\gamma}\frac{\Omega^2}{(\hbar\Omega-\varepsilon_{mn})^2+\varsigma^2}\Delta_{mn}^{\alpha}\Omega_{mn}^{\beta\gamma}g_{mn}\\ &= -\pi\nu_c\hbar\int[d\boldsymbol{k}]\sum_{m\neq n}\frac{\Omega^2}{(\hbar\Omega-\varepsilon_{mn})^2+\varsigma^2}\Delta_{mn}^{\alpha}\Omega_{mn}^{\alpha_1\alpha_2}g_{mn}.\end{aligned} \tag{E38}$$

The second term in Eq. (E37) is

$$\kappa_{\mathrm{ee,d},2}^{\alpha\alpha_1\alpha_2} = -\lim_{\omega\to0}\frac{i\nu_c\hbar}{\omega}\int[d\boldsymbol{k}]\sum_{m\neq n}E_A^{\alpha_1\alpha_2\beta\gamma}\mathrm{P}\frac{1}{\hbar\Omega-\varepsilon_{mn}}\Omega^2\Delta_{mp}^{\alpha}G_{mn}^{\beta\gamma}g_{mn}. \tag{E39}$$

Noting that in the CP responses $\beta\neq\gamma$, $E_A^{\alpha_1\alpha_2\beta\gamma}=-E_A^{\alpha_1\alpha_2\gamma\beta}$, and making use of the fact that $G_{mn}^{\beta\gamma}=G_{mn}^{\gamma\beta}$, we have $\kappa_{\mathrm{ee,d},2}^{\alpha\alpha_1\alpha_2}=0$. The third term in Eq. (E37) is written as

$$\begin{aligned}\kappa_{\mathrm{Rec},1}^{\alpha\alpha_1\alpha_2} &= \frac{i\nu_c\hbar}{2\omega}\int[d\boldsymbol{k}]\sum_{m\neq n}\frac{\omega}{(\hbar\Omega-\varepsilon_{mn})^2}\Omega^2\Delta_{mp}^{\alpha}\left(\mathcal{A}_{mn}^{\alpha_1}\mathcal{A}_{nm}^{\alpha_2}-\mathcal{A}_{mn}^{\alpha_2}\mathcal{A}_{nm}^{\alpha_1}\right)g_{mn}\\ &= \frac{\nu_c\hbar}{2}\int[d\boldsymbol{k}]\sum_{m\neq n}\frac{\Omega^2}{(\hbar\Omega-\varepsilon_{mn})^2}\Delta_{mp}^{\alpha}\Omega_{mn}^{\alpha_1\alpha_2}g_{mn}\\ &= -\frac{\nu_c\hbar}{2}\int[d\boldsymbol{k}]\sum_{m\neq n}\partial^{\alpha}\left(\frac{1}{\hbar\Omega-\varepsilon_{mn}}\right)\Omega^2\Omega_{mn}^{\alpha_1\alpha_2}g_{mn}.\end{aligned} \tag{E40}$$

We will show in the following that $\kappa_{\mathrm{Rec},1}^{\alpha\alpha_1\alpha_2}$ is a part of the CP rectification current.

4. Shift spin current

Now we consider the remaining terms $\chi_{\rm ie}$ and the nondiagonal component of $\chi_{\rm ee}$, which is denoted as $\chi_{\rm ee,od}$. We show that the summation of these two terms comprises the shift current. With use of used partial integration, $\chi_{\rm ie}$ can be rewritten as

$$\begin{aligned}\chi_{\rm ie}^{\alpha\alpha_1\alpha_2} &= \lim_{\omega\to 0}\frac{\nu_c}{2}\int[d\boldsymbol{k}]\sum_{m\neq n}\epsilon^{\alpha_1 z\beta}\epsilon^{\alpha_2 z\gamma}\omega_1\omega_2\big[-\partial^\beta\mathcal{A}^\alpha_{mn}+i\big(\mathcal{A}^\beta_{nn}-\mathcal{A}^\beta_{mm}\big)\mathcal{A}^\alpha_{mn}\big]d_{nm}(\omega_2)\mathcal{A}^\gamma_{nm}g_{nm}+[(\alpha_1,\omega_1)\leftrightarrow(\alpha_2,\omega_2)]\\ &= \lim_{\omega\to 0}\frac{\nu_c}{2}\int[d\boldsymbol{k}]\sum_{m\neq n}\left(\epsilon^{\alpha_1 z\beta}\epsilon^{\alpha_2 z\gamma}\frac{1}{-\hbar\Omega-\varepsilon_{nm}}+\epsilon^{\alpha_2 z\beta}\epsilon^{\alpha_1 z\gamma}\frac{1}{\hbar\omega+\hbar\Omega-\varepsilon_{nm}}\right)\\ &\quad\times\omega_1\omega_2\big[-\partial^\beta\mathcal{A}^\alpha_{mn}+i\big(\mathcal{A}^\beta_{nn}-\mathcal{A}^\beta_{mm}\big)\mathcal{A}^\alpha_{mn}\big]\mathcal{A}^\gamma_{nm}g_{nm}.\end{aligned}\tag{E41}$$

Note that

$$\partial^\beta\mathcal{A}^\alpha_{mn}-i\big(\mathcal{A}^\beta_{nn}-\mathcal{A}^\beta_{mm}\big)\mathcal{A}^\alpha_{mn}=[D^\beta\mathcal{A}^\alpha]_{mn}.\tag{E42}$$

Making use of Eqs. (E26) and (E27), the LP-photocurrent tensor is obtained as

$$\begin{aligned}\eta_{\rm ie}^{\alpha\alpha_1\alpha_2} &= -\lim_{\omega\to 0}\frac{\nu_c}{2}\int[d\boldsymbol{k}]\sum_{m\neq n}E_S^{\alpha_1\alpha_2\beta\gamma}\left(\frac{1}{-\hbar\Omega-\varepsilon_{nm}}[D^\beta\mathcal{A}^\alpha]_{mn}\mathcal{A}^\gamma_{nm}-\frac{1}{\hbar\omega+\hbar\Omega+\varepsilon_{nm}}[D^\beta\mathcal{A}^\alpha]_{nm}\mathcal{A}^\gamma_{mn}\right)\Omega(\omega+\Omega)g_{nm}\\ &= \frac{\nu_c}{2}\int[d\boldsymbol{k}]\sum_{m\neq n}E_S^{\alpha_1\alpha_2\beta\gamma}\mathrm{P}\frac{1}{\hbar\Omega-\varepsilon_{mn}}\Omega^2\big([D^\beta\mathcal{A}^\alpha]_{mn}\mathcal{A}^\gamma_{nm}+[D^\beta\mathcal{A}^\alpha]_{nm}\mathcal{A}^\gamma_{mn}\big)g_{nm}\\ &\quad+i\frac{\pi\nu_c}{2}\int[d\boldsymbol{k}]\sum_{m\neq n}E_S^{\alpha_1\alpha_2\beta\gamma}\delta(\hbar\Omega-\varepsilon_{mn})\Omega^2\big([D^\beta\mathcal{A}^\alpha]_{mn}\mathcal{A}^\gamma_{nm}-[D^\beta\mathcal{A}^\alpha]_{nm}\mathcal{A}^\gamma_{mn}\big)g_{nm}.\end{aligned}\tag{E43}$$

The CP-photocurrent tensor is

$$\begin{aligned}\kappa_{\rm ie}^{\alpha\alpha_1\alpha_2} &= \lim_{\omega\to 0}\frac{i\nu_c}{2}\int[d\boldsymbol{k}]\sum_{m\neq n}E_A^{\alpha_1\alpha_2\beta\gamma}\left(\frac{1}{-\hbar\Omega-\varepsilon_{nm}}[D^\beta\mathcal{A}^\alpha]_{mn}\mathcal{A}^\gamma_{nm}+\frac{1}{\hbar\omega+\hbar\Omega+\varepsilon_{nm}}[D^\beta\mathcal{A}^\alpha]_{nm}\mathcal{A}^\gamma_{mn}\right)\Omega(\omega+\Omega)g_{nm}\\ &= \frac{\pi\nu_c}{2}\int[d\boldsymbol{k}]\sum_{m\neq n}E_A^{\alpha_1\alpha_2\beta\gamma}\delta(\hbar\Omega-\varepsilon_{mn})\Omega^2\big([D^\beta\mathcal{A}^\alpha]_{mn}\mathcal{A}^\gamma_{nm}+[D^\beta\mathcal{A}^\alpha]_{nm}\mathcal{A}^\gamma_{mn}\big)g_{nm}\\ &\quad-\frac{i\nu_c}{2}\int[d\boldsymbol{k}]\sum_{m\neq n}E_A^{\alpha_1\alpha_2\beta\gamma}\mathrm{P}\frac{1}{\hbar\Omega-\varepsilon_{mn}}\Omega^2\big([D^\beta\mathcal{A}^\alpha]_{mn}\mathcal{A}^\gamma_{nm}-[D^\beta\mathcal{A}^\alpha]_{nm}\mathcal{A}^\gamma_{mn}\big)g_{nm}.\end{aligned}\tag{E44}$$

Now we consider the remaining component of $\chi_{\rm ee}$, which is denoted as $\chi_{\rm ee,od}$,

$$\begin{aligned}\chi_{\rm ee,od}^{\alpha\alpha_1\alpha_2} &= \lim_{\omega\to 0}i\frac{\nu_c}{2}\int[d\boldsymbol{k}]\sum_{m\neq n\neq p}\epsilon^{\alpha_1 z\beta}\epsilon^{\alpha_2 z\gamma}\omega_1\omega_2\mathcal{A}^\alpha_{mn}\big[d_{pm}(\omega_2)\mathcal{A}^\beta_{np}\mathcal{A}^\gamma_{pm}g_{mp}-d_{np}(\omega_2)\mathcal{A}^\beta_{pm}\mathcal{A}^\gamma_{np}g_{pn}\big]+[(\alpha_1,\omega_1)\leftrightarrow(\alpha_2,\omega_2)]\\ &= \lim_{\omega\to 0}i\frac{\nu_c}{2}\int[d\boldsymbol{k}]\sum_{m\neq n\neq p}\epsilon^{\alpha_1 z\beta}\epsilon^{\alpha_2 z\gamma}\omega_1\omega_2\big(\mathcal{A}^\alpha_{mn}\mathcal{A}^\beta_{np}-\mathcal{A}^\beta_{mn}\mathcal{A}^\alpha_{np}\big)d_{pm}(\omega_2)\mathcal{A}^\gamma_{pm}g_{mp}+[(\alpha_1,\omega_1)\leftrightarrow(\alpha_2,\omega_2)]\\ &= \lim_{\omega\to 0}i\frac{\nu_c}{2}\int[d\boldsymbol{k}]\sum_{m\neq n\neq p}\left(\epsilon^{\alpha_1 z\beta}\epsilon^{\alpha_2 z\gamma}\frac{1}{-\hbar\Omega-\varepsilon_{pm}}+\epsilon^{\alpha_2 z\beta}\epsilon^{\alpha_1 z\gamma}\frac{1}{\hbar\omega+\hbar\Omega-\varepsilon_{pm}}\right)\Omega(\omega+\Omega)\big(\mathcal{A}^\alpha_{mn}\mathcal{A}^\beta_{np}-\mathcal{A}^\beta_{mn}\mathcal{A}^\alpha_{np}\big)\mathcal{A}^\gamma_{pm}g_{mp}\\ &= \lim_{\omega\to 0}\frac{\nu_c}{2}\int[d\boldsymbol{k}]\sum_{m\neq p}\left(\epsilon^{\alpha_1 z\beta}\epsilon^{\alpha_2 z\gamma}\frac{1}{-\hbar\Omega-\varepsilon_{pm}}+\epsilon^{\alpha_2 z\beta}\epsilon^{\alpha_1 z\gamma}\frac{1}{\hbar\omega+\hbar\Omega-\varepsilon_{pm}}\right)\Omega(\omega+\Omega)([D^\alpha\mathcal{A}^\beta]_{mp}-[D^\beta\mathcal{A}^\alpha]_{mp})\mathcal{A}^\gamma_{pm}g_{mp},\end{aligned}\tag{E45}$$

where in the last equality the relation $\sum_{n\neq m,p}(\mathcal{A}^\alpha_{mn}\mathcal{A}^\beta_{np}-\mathcal{A}^\beta_{mn}\mathcal{A}^\alpha_{np})=-i([D^\alpha\mathcal{A}^\beta]_{mp}-[D^\beta\mathcal{A}^\alpha]_{mp})$ is used. For notational simplicity, we denote $K^{\alpha\beta\gamma}_{mp}=([D^\alpha\mathcal{A}^\beta]_{mp}-[D^\beta\mathcal{A}^\alpha]_{mp})\mathcal{A}^\gamma_{pm}$, and the LP response of $\chi^{\alpha\alpha_1\alpha_2}_{\rm ee,od}$ is written as

$$\begin{aligned}\eta_{\rm ee,od}^{\alpha\alpha_1\alpha_2} &= \lim_{\omega\to 0}\frac{\nu_c}{2}\int[d\boldsymbol{k}]\sum_{m\neq p}E_S^{\alpha_1\alpha_2\beta\gamma}\left(\frac{1}{-\hbar\Omega-\varepsilon_{pm}}+\frac{1}{\hbar\omega+\hbar\Omega-\varepsilon_{pm}}\right)\Omega(\omega+\Omega)K^{\alpha\beta\gamma}_{mp}g_{mp}\\ &= \lim_{\omega\to 0}\frac{\nu_c}{2}\int[d\boldsymbol{k}]\sum_{m\neq p}E_S^{\alpha_1\alpha_2\beta\gamma}\left(\frac{1}{-\hbar\Omega-\varepsilon_{pm}}K^{\alpha\beta\gamma}_{mp}-\frac{1}{\hbar\omega+\hbar\Omega+\varepsilon_{pm}}K^{\alpha\beta\gamma}_{pm}\right)\Omega^2 g_{mp}\end{aligned}$$

$$= -\frac{\nu_c}{2}\int [d\boldsymbol{k}]\sum_{m\neq p} E_S^{\alpha_1\alpha_2\beta\gamma}\mathrm{P}\frac{1}{\hbar\Omega-\varepsilon_{mp}}\left(K_{mp}^{\alpha\beta\gamma}+K_{pm}^{\alpha\beta\gamma}\right)\Omega^2 g_{mp}$$
$$-i\frac{\pi\nu_c}{2}\int [d\boldsymbol{k}]\sum_{m\neq p} E_S^{\alpha_1\alpha_2\beta\gamma}\delta(\hbar\Omega-\varepsilon_{mp})\left(K_{mp}^{\alpha\beta\gamma}-K_{pm}^{\alpha\beta\gamma}\right)\Omega^2 g_{mp}. \tag{E46}$$

Adding Eqs. (E43) and (E46) yields

$$\begin{aligned}\eta_{\mathrm{ie}}^{\alpha\alpha_1\alpha_2}+\eta_{\mathrm{ee,od}}^{\alpha\alpha_1\alpha_2} =& -i\frac{\pi\nu_c}{2}\int [d\boldsymbol{k}]\sum_{m\neq n} E_S^{\alpha_1\alpha_2\beta\gamma}\Omega^2\delta(\hbar\Omega-\varepsilon_{mn})\left([D^\alpha\mathcal{A}^\beta]_{mn}\mathcal{A}^\gamma_{nm}-[D^\alpha\mathcal{A}^\beta]_{nm}\mathcal{A}^\gamma_{mn}\right)g_{mn}\\ &-\frac{\nu_c}{2}\int [d\boldsymbol{k}]\sum_{m\neq n} E_S^{\alpha_1\alpha_2\beta\gamma}\Omega^2\mathrm{P}\frac{1}{\hbar\Omega-\varepsilon_{mn}}\left([D^\alpha\mathcal{A}^\beta]_{mn}\mathcal{A}^\gamma_{nm}+[D^\alpha\mathcal{A}^\beta]_{nm}\mathcal{A}^\gamma_{mn}\right)g_{mn}\\ =& -i\varsigma\frac{\pi\nu_c}{2}\int [d\boldsymbol{k}]\sum_{m\neq n}\Omega^2\delta(\hbar\Omega-\varepsilon_{mn})\left([D^\alpha\mathcal{A}^{\alpha_1}]_{mn}\mathcal{A}^{\alpha_2}_{nm}-[D^\alpha\mathcal{A}^{\alpha_1}]_{nm}\mathcal{A}^{\alpha_2}_{mn}\right.\\ &\left.+[D^\alpha\mathcal{A}^{\alpha_2}]_{mn}\mathcal{A}^{\alpha_1}_{nm}-[D^\alpha\mathcal{A}^{\alpha_2}]_{nm}\mathcal{A}^{\alpha_1}_{mn}\right)g_{mn}\\ &-\varsigma\frac{\nu_c}{2}\int [d\boldsymbol{k}]\sum_{m\neq n}\Omega^2\mathrm{P}\frac{1}{\hbar\Omega-\varepsilon_{mn}}\left([D^\alpha\mathcal{A}^{\alpha_1}]_{mn}\mathcal{A}^{\alpha_2}_{nm}+[D^\alpha\mathcal{A}^{\alpha_1}]_{nm}\mathcal{A}^{\alpha_2}_{mn}+[D^\alpha\mathcal{A}^{\alpha_2}]_{mn}\mathcal{A}^{\alpha_1}_{nm}+[D^\alpha\mathcal{A}^{\alpha_2}]_{nm}\mathcal{A}^{\alpha_1}_{mn}\right)g_{mn}.\end{aligned} \tag{E47}$$

Making use of the relation

$$[D^\alpha\mathcal{A}^{\alpha_1}]_{mn}\mathcal{A}^{\alpha_2}_{nm}=\left([D^\alpha\mathcal{A}^{\alpha_1}]_{nm}\mathcal{A}^{\alpha_2}_{mn}\right)^*, \tag{E48}$$

we have

$$\begin{aligned}\eta_{\mathrm{ie}}^{\alpha\alpha_1\alpha_2}+\eta_{\mathrm{ee,od}}^{\alpha\alpha_1\alpha_2} =& \varsigma\pi\nu_c\int [d\boldsymbol{k}]\sum_{m\neq n}\Omega^2\delta(\hbar\Omega-\varepsilon_{mn})\mathrm{Im}\left([D^\alpha\mathcal{A}^{\alpha_1}]_{mn}\mathcal{A}^{\alpha_2}_{nm}+[D^\alpha\mathcal{A}^{\alpha_2}]_{mn}\mathcal{A}^{\alpha_1}_{nm}\right)g_{mn}\\ &-\varsigma\nu_c\int [d\boldsymbol{k}]\sum_{m\neq n}\Omega^2\mathrm{P}\frac{1}{\hbar\Omega-\varepsilon_{mn}}\mathrm{Re}\left([D^\alpha\mathcal{A}^{\alpha_1}]_{mn}\mathcal{A}^{\alpha_2}_{nm}+[D^\alpha\mathcal{A}^{\alpha_2}]_{mn}\mathcal{A}^{\alpha_1}_{nm}\right)g_{mn}.\end{aligned} \tag{E49}$$

The first term in Eq. (E49) is the shift current. Following Refs. [65,67], we define the shift vector:

$$R^{\alpha_1\alpha_2}_{mn}=\mathcal{A}^{\alpha_1}_{mm}-\mathcal{A}^{\alpha_1}_{nn}-\partial^{\alpha_1}\arg\mathcal{A}^{\alpha_2}_{mn}. \tag{E50}$$

We can write the LP-shift current in terms of the magnon shift vector as

$$\begin{aligned}\eta_{\mathrm{Sh}}^{\alpha\alpha_1\alpha_2} =& \frac{\pi\nu_c}{2}\int [d\boldsymbol{k}]\sum_{m\neq n}\Omega^2\delta(\hbar\Omega-\varepsilon_{mn})\left(R^{\alpha\alpha_1}_{mn}+R^{\alpha\alpha_2}_{mn}\right)G^{\alpha_1\alpha_2}_{mn}g_{mn}\\ &-\frac{\pi\nu_c}{2}\int [d\boldsymbol{k}]\sum_{m\neq n}\Omega^2\delta(\hbar\Omega-\varepsilon_{mn})\left(\left|\mathcal{A}^{\alpha_2}_{nm}\right|\partial^\alpha\left|\mathcal{A}^{\alpha_1}_{mn}\right|-\left|\mathcal{A}^{\alpha_1}_{mn}\right|\partial^\alpha\left|\mathcal{A}^{\alpha_2}_{nm}\right|\right)\sin\left(\phi^{\alpha_1}_{mn}+\phi^{\alpha_2}_{nm}\right)g_{mn}.\end{aligned} \tag{E51}$$

It describes the current generated by the shift of the magnon position in the interband transition from band m to n. One can verify that the shift current is invariant to the gauge transformation with use of the relation

$$\mathrm{Re}\left([D^\alpha\mathcal{A}^{\alpha_1}]_{mn}\mathcal{A}^{\alpha_2}_{nm}+[D^\alpha\mathcal{A}^{\alpha_2}]_{mn}\mathcal{A}^{\alpha_1}_{nm}\right)=\partial^\alpha G^{\alpha_1\alpha_2}_{mn}. \tag{E52}$$

The second term in Eq. (E49) is part of the rectification current, which is written as

$$\eta_{\mathrm{Rec},2}^{\alpha\alpha_1\alpha_2}=-\varsigma 2\nu_c\int [d\boldsymbol{k}]\sum_{m\neq n}\Omega^2\mathrm{P}\frac{1}{\hbar\Omega-\varepsilon_{mn}}\partial^\alpha G^{\alpha_1\alpha_2}_{mn}g_{mn}. \tag{E53}$$

Combining Eqs. (E35) and (E53), we have

$$\eta_{\mathrm{Rec}}^{\alpha\alpha_1\alpha_2}=\eta_{\mathrm{Rec},1}^{\alpha\alpha_1\alpha_2}+\eta_{\mathrm{Rec},2}^{\alpha\alpha_1\alpha_2}=2\nu_c\int [d\boldsymbol{k}]\sum_{m\neq n}\Omega^2\frac{1}{\hbar\Omega-\varepsilon_{mn}}G^{\alpha_1\alpha_2}_{mn}\partial^\alpha g_{mn}. \tag{E54}$$

The CP-photocurrent tensor is

$$\begin{aligned}\kappa_{\mathrm{ee,od}}^{\alpha\alpha_1\alpha_2} &= \lim_{\omega\to 0} i\frac{\nu_c}{2}\int [d\boldsymbol{k}]\sum_{m\neq p} E_A^{\alpha_1\alpha_2\beta\gamma}\left(\frac{1}{-\hbar\Omega-\varepsilon_{pm}}-\frac{1}{\hbar\omega+\hbar\Omega-\varepsilon_{pm}}\right)\Omega(\omega+\Omega)([D^\alpha\mathcal{A}^\beta]_{mp}-[D^\beta\mathcal{A}^\alpha]_{mp})\mathcal{A}^\gamma_{pm}g_{mp}\\ &= \lim_{\omega\to 0} i\frac{\nu_c}{2}\int [d\boldsymbol{k}]\sum_{m\neq p} E_S^{\alpha_1\alpha_2\beta\gamma}\left(\frac{1}{-\hbar\Omega-\varepsilon_{pm}}K^{\alpha\beta\gamma}_{mp}+\frac{1}{\hbar\omega+\hbar\Omega+\varepsilon_{pm}}K^{\alpha\beta\gamma}_{pm}\right)\Omega^2 g_{mp}\\ &= -i\frac{\nu_c}{2}\int [d\boldsymbol{k}]\sum_{m\neq p} E_S^{\alpha_1\alpha_2\beta\gamma}\mathrm{P}\frac{1}{\hbar\Omega-\varepsilon_{mn}}\left(K^{\alpha\beta\gamma}_{mp}-K^{\alpha\beta\gamma}_{pm}\right)\Omega^2 g_{mp}\\ &\quad+\frac{\pi\nu_c}{2}\int [d\boldsymbol{k}]\sum_{m\neq p} E_A^{\alpha_1\alpha_2\beta\gamma}\delta(\hbar\Omega-\varepsilon_{mn})\left[K^{\alpha\beta\gamma}_{mp}+K^{\alpha\beta\gamma}_{pm}\right]\Omega^2 g_{mp}.\end{aligned}\tag{E55}$$

Adding Eqs. (E44) and (E55), we have

$$\begin{aligned}\kappa_{\mathrm{ee,od}}^{\alpha\alpha_1\alpha_2}+\kappa_{\mathrm{ie}}^{\alpha\alpha_1\alpha_2} &= -i\frac{\nu_c}{2}\int [d\boldsymbol{k}]\sum_{m\neq p} E_S^{\alpha_1\alpha_2\beta\gamma}\mathrm{P}\frac{1}{\hbar\Omega-\varepsilon_{mn}}\left([D^\alpha\mathcal{A}^\beta]_{mp}\mathcal{A}^\gamma_{pm}-[D^\alpha\mathcal{A}^\beta]_{pm}\mathcal{A}^\gamma_{mp}\right)\Omega^2 g_{mp}\\ &\quad+\frac{\pi\nu_c}{2}\int [d\boldsymbol{k}]\sum_{m\neq p} E_A^{\alpha_1\alpha_2\beta\gamma}\delta(\hbar\Omega-\varepsilon_{mn})\left([D^\alpha\mathcal{A}^\beta]_{mp}\mathcal{A}^\gamma_{pm}+[D^\alpha\mathcal{A}^\beta]_{pm}\mathcal{A}^\gamma_{mp}\right)\Omega^2 g_{mp}\\ &= -\frac{\pi\nu_c}{2}\int [d\boldsymbol{k}]\sum_{m\neq p}\delta(\hbar\Omega-\varepsilon_{mn})\left([D^\alpha\mathcal{A}^{\alpha_1}]_{mp}\mathcal{A}^{\alpha_2}_{pm}+[D^\alpha\mathcal{A}^{\alpha_1}]_{pm}\mathcal{A}^{\alpha_2}_{mp}\right.\\ &\quad\left.-[D^\alpha\mathcal{A}^{\alpha_2}]_{mp}\mathcal{A}^{\alpha_1}_{pm}-[D^\alpha\mathcal{A}^{\alpha_2}]_{pm}\mathcal{A}^{\alpha_1}_{mp}\right)\Omega^2 g_{mp}+i\frac{\nu_c}{2}\int [d\boldsymbol{k}]\sum_{m\neq p}\mathrm{P}\frac{1}{\hbar\Omega-\varepsilon_{mn}}\left([D^\alpha\mathcal{A}^{\alpha_1}]_{mp}\mathcal{A}^{\alpha_2}_{pm}\right.\\ &\quad\left.-[D^\alpha\mathcal{A}^{\alpha_1}]_{pm}\mathcal{A}^{\alpha_2}_{mp}-[D^\alpha\mathcal{A}^{\alpha_2}]_{mp}\mathcal{A}^{\alpha_1}_{pm}+[D^\alpha\mathcal{A}^{\alpha_2}]_{pm}\mathcal{A}^{\alpha_1}_{mp}\right)\Omega^2 g_{mp}.\end{aligned}\tag{E56}$$

Using Eqs. (E48) and (E52), we have

$$\begin{aligned}\kappa_{\mathrm{ee,od}}^{\alpha\alpha_1\alpha_2}+\kappa_{\mathrm{ie}}^{\alpha\alpha_1\alpha_2} &= -\frac{\pi\nu_c}{2}\int [d\boldsymbol{k}]\sum_{m\neq p}\delta(\hbar\Omega-\varepsilon_{mn})\mathrm{Re}\left([D^\alpha\mathcal{A}^{\alpha_1}]_{mp}\mathcal{A}^{\alpha_2}_{pm}-[D^\alpha\mathcal{A}^{\alpha_2}]_{mp}\mathcal{A}^{\alpha_1}_{pm}\right)\Omega^2 g_{mp}\\ &\quad-\frac{\nu_c}{2}\int [d\boldsymbol{k}]\sum_{m\neq p}\mathrm{P}\frac{1}{\hbar\Omega-\varepsilon_{mn}}\mathrm{Im}\left([D^\alpha\mathcal{A}^{\alpha_1}]_{mp}\mathcal{A}^{\alpha_2}_{pm}-[D^\alpha\mathcal{A}^{\alpha_2}]_{mp}\mathcal{A}^{\alpha_1}_{pm}\right)\Omega^2 g_{mp}.\end{aligned}\tag{E57}$$

Inheriting the concept from the electron photocurrent responses, the first term in Eq. (E57) is the CP shift current:

$$\kappa_{\mathrm{Sh}}^{\alpha\alpha_1\alpha_2}=-\frac{\pi\nu_c}{2}\int [d\boldsymbol{k}]\sum_{m\neq p}\delta(\hbar\Omega-\varepsilon_{mn})\mathrm{Re}\left([D^\alpha\mathcal{A}^{\alpha_1}]_{mp}\mathcal{A}^{\alpha_2}_{pm}-[D^\alpha\mathcal{A}^{\alpha_2}]_{mp}\mathcal{A}^{\alpha_1}_{pm}\right)\Omega^2 g_{mp}.\tag{E58}$$

Introducing the chiral shift vector,

$$R^{\alpha,\pm}_{mn}=\mathcal{A}^\alpha_{mm}-\mathcal{A}^\alpha_{nn}-\partial^\alpha\arg\mathcal{A}^\pm_{mn},\tag{E59}$$

with use of the circular representation of the Berry connection $\mathcal{A}^\pm_{mn}=\frac{1}{\sqrt{2}}(\mathcal{A}^x_{mn}\pm i\mathcal{A}^y_{mn})$, Eq. (E58) can be rewritten as

$$\kappa_{\mathrm{Sh}}^{\alpha\alpha_1\alpha_2}=-\frac{\pi\nu_c}{2}\int [d\boldsymbol{k}]\sum_{m\neq n}\Omega^2\delta(\hbar\Omega-\varepsilon_{mn})\left(R^{\alpha,+}_{mn}|\mathcal{A}^+_{nm}|^2-R^{\alpha,-}_{mn}|\mathcal{A}^-_{nm}|^2\right)g_{mn}\tag{E60}$$

with use of the relation

$$\mathrm{Im}\left([D^\alpha\mathcal{A}^{\alpha_1}]_{mp}\mathcal{A}^{\alpha_2}_{pm}-[D^\alpha\mathcal{A}^{\alpha_2}]_{mp}\mathcal{A}^{\alpha_1}_{pm}\right)=-\tfrac{1}{2}\partial^\alpha\Omega^{\alpha_1\alpha_2}_{mn}.\tag{E61}$$

The second term in Eq. (E57) is a part of the CP rectification current, which is written as

$$\kappa_{\mathrm{Rec},2}^{\alpha\alpha_1\alpha_2}=\frac{\nu_c}{2}\int [d\boldsymbol{k}]\sum_{m\neq n}\mathrm{P}\frac{1}{\hbar\Omega-\varepsilon_{mn}}\Omega^2\partial^\alpha\Omega^{\alpha_1\alpha_2}_{mn}g_{mn}.\tag{E62}$$

Combining Eqs. (E40) and (E62), we have

$$\kappa_{\mathrm{Rec}}^{\alpha\alpha_1\alpha_2}=\kappa_{\mathrm{Rec},1}^{\alpha\alpha_1\alpha_2}+\kappa_{\mathrm{Rec},2}^{\alpha\alpha_1\alpha_2}=\frac{\nu_c}{2}\int [d\boldsymbol{k}]\sum_{m\neq n}\frac{\Omega^2}{\hbar\Omega-\varepsilon_{mn}}\Omega^{\alpha_1\alpha_2}_{mn}\partial^\alpha g_{mn}.\tag{E63}$$

In conclusion, the magnon spin photocurrent is expressed in terms of the following gauge invariant quantities:

$$v_m^\alpha = \frac{1}{\hbar}\partial^\alpha \varepsilon_m, \quad \Delta_{mn}^\alpha = v_m^\alpha - v_n^\alpha, \tag{E64}$$

$$\Omega_m^\tau = \frac{i}{2}\epsilon^{\alpha\gamma\tau}\sum_{n\neq m}\left(\mathcal{A}_{mn}^\alpha \mathcal{A}_{nm}^\gamma - \mathcal{A}_{mn}^\gamma \mathcal{A}_{nm}^\alpha\right), \tag{E65}$$

$$\Omega_{mn}^{\beta\gamma} = i\left(\mathcal{A}_{mn}^\beta \mathcal{A}_{nm}^\gamma - \mathcal{A}_{mn}^\gamma \mathcal{A}_{nm}^\beta\right), \tag{E66}$$

$$G_{mn}^{\beta\gamma} = \frac{1}{2}\left(\mathcal{A}_{mn}^\beta \mathcal{A}_{nm}^\gamma + \mathcal{A}_{mn}^\gamma \mathcal{A}_{nm}^\beta\right), \tag{E67}$$

$$R_{mn}^{\alpha\alpha_1} = \mathcal{A}_{mm}^\alpha - \mathcal{A}_{nn}^\alpha - \partial^\alpha \arg \mathcal{A}_{mn}^{\alpha_1}, \tag{E68}$$

$$R_{mn}^{\alpha,\pm} = \mathcal{A}_{mm}^\alpha - \mathcal{A}_{nn}^\alpha - \partial^\alpha \arg \mathcal{A}_{mn}^{\pm}, \tag{E69}$$

where v_m^α is the group velocity, Ω_m^τ is the Berry curvature for the mth band, $\Omega_{mn}^{\beta\gamma}$ is the band-resolved Berry curvature, $G_{mn}^{\beta\gamma}$ is the band-resolved quantum metric, and $R_{mn}^{\alpha_1\alpha_2}$ is the shift vector, $R_{mn}^{\alpha,\pm}$ is the chiral shift vector with the Berry connection in circular representation $\mathcal{A}_{mn}^\pm = \frac{1}{\sqrt{2}}(\mathcal{A}_{mn}^x \pm i\mathcal{A}_{mn}^y)$. The magnon spin photocurrent is composed of five distinct parts: Drude current, Berry curvature dipole (BCD) current, injection current, shift current, and the rectification current:

$$\eta_{\mathrm{D}}^{\alpha\alpha_1\alpha_2} = \varsigma\frac{\nu_c}{\hbar}\int [d\boldsymbol{k}]\sum_m v_m^\alpha \partial^{\alpha_1}\partial^{\alpha_2} g_m, \tag{E70}$$

$$\kappa_{\mathrm{BCD}}^{\alpha\alpha_1\alpha_2} = \frac{\nu_c\Omega}{2\hbar}\int [d\boldsymbol{k}]\sum_m (\epsilon^{\alpha\alpha_2\tau}\partial^{\alpha_1} - \epsilon^{\alpha\alpha_1\tau}\partial^{\alpha_2})\Omega_m^\tau g_m, \tag{E71}$$

$$\eta_{\mathrm{Inj}}^{\alpha\alpha_1\alpha_2} = -\varsigma 2\hbar\nu_c\int [d\boldsymbol{k}]\sum_{m\neq n}\frac{\Omega^2}{(\hbar\Omega - \varepsilon_{mn})^2 + \varsigma^2}\Delta_{mn}^\alpha G_{mn}^{\alpha_1\alpha_2} g_{mn}, \tag{E72}$$

$$\kappa_{\mathrm{Inj}}^{\alpha\alpha_1\alpha_2} = -\pi\nu_c\hbar\int [d\boldsymbol{k}]\sum_{m\neq n}\frac{\Omega^2}{(\hbar\Omega - \varepsilon_{mn})^2 + \varsigma^2}\Delta_{mn}^\alpha \Omega_{mn}^{\alpha_1\alpha_2} g_{mn}, \tag{E73}$$

$$\eta_{\mathrm{Sh}}^{\alpha\alpha_1\alpha_1} = \varsigma\pi\nu_c\int [d\boldsymbol{k}]\sum_{m\neq n}\Omega^2\delta(\hbar\Omega - \varepsilon_{mn})R_{mn}^{\alpha\alpha_1}G_{mn}^{\alpha_1\alpha_1} g_{mn}, \tag{E74}$$

$$\kappa_{\mathrm{Sh}}^{\alpha\alpha_1\alpha_2} = -\frac{\pi\nu_c}{2}\int [d\boldsymbol{k}]\sum_{m\neq n}\Omega^2\delta(\hbar\Omega - \varepsilon_{mn})\left(R_{mn}^{\alpha,+}|\mathcal{A}_{nm}^+|^2 - R_{mn}^{\alpha,-}|\mathcal{A}_{nm}^-|^2\right) g_{mn}, \tag{E75}$$

$$\eta_{\mathrm{Rec}}^{\alpha\alpha_1\alpha_1} = \varsigma 2\nu_c\int [d\boldsymbol{k}]\sum_{m\neq n}\frac{\Omega^2}{\hbar\Omega - \varepsilon_{mn}}G_{mn}^{\alpha_1\alpha_2}\partial^\alpha g_{mn}, \tag{E76}$$

$$\kappa_{\mathrm{Rec}}^{\alpha\alpha_1\alpha_1} = -\frac{\nu_c}{2}\int [d\boldsymbol{k}]\sum_{m\neq n}\frac{\Omega^2}{\hbar\Omega - \varepsilon_{mn}}\Omega_{mn}^{\alpha_1\alpha_2}\partial^\alpha g_{mn}, \tag{E77}$$

in which $\varsigma = 1$ for $\alpha_1 = \alpha_2$ and $\varsigma = -1$ for $\alpha_1 \neq \alpha_2$.

5. Some derivations for the symmetry analysis

According to Eq. (D9), the element of the Berry connection matrix is

$$\mathcal{A}_{\boldsymbol{k}mn}^\alpha = i\sum_p (U_{\boldsymbol{k}}^\dagger)_{mp}\frac{\partial (U_{\boldsymbol{k}})_{pn}}{\partial k_\alpha} = i\sum_p U_{\boldsymbol{k}pm}^*\frac{\partial U_{\boldsymbol{k}pn}}{\partial k_\alpha}. \tag{E78}$$

The $\mathcal{T}'$ symmetry gives a constraint on the Berry connection

$$\mathcal{A}_{\boldsymbol{k}mn}^\alpha = i\sum_p (U_{-\boldsymbol{k}}^*)_{mp}\frac{\partial \left(U_{-\boldsymbol{k}}^T\right)_{pn}}{\partial k_\alpha} = i\sum_p U_{-\boldsymbol{k}pm}^*\frac{\partial U_{-\boldsymbol{k}np}}{\partial k_\alpha} = \mathcal{A}_{-\boldsymbol{k}nm}^\alpha. \tag{E79}$$

With use of Eq. (E79), the Berry curvature satisfies the relation [see Eq. (E65)]

$$\Omega_{\boldsymbol{k}m}^\tau = \frac{i}{2}\epsilon^{\alpha\gamma\tau}\sum_{n\neq m}\left(\mathcal{A}_{\boldsymbol{k}mn}^\alpha \mathcal{A}_{\boldsymbol{k}nm}^\gamma - \mathcal{A}_{\boldsymbol{k}mn}^\gamma \mathcal{A}_{\boldsymbol{k}nm}^\alpha\right) = \frac{i}{2}\epsilon^{\alpha\gamma\tau}\sum_{n\neq m}\left(\mathcal{A}_{-\boldsymbol{k}nm}^\alpha \mathcal{A}_{-\boldsymbol{k}mn}^\gamma - \mathcal{A}_{-\boldsymbol{k}nm}^\gamma \mathcal{A}_{-\boldsymbol{k}mn}^\alpha\right) = -\Omega_{-\boldsymbol{k}m}^\tau. \tag{E80}$$

For the point-group symmetry transformations $\mathcal{M}$, with eigenvalues $\varepsilon_{n\boldsymbol{k}} = \varepsilon_{n\mathcal{M}^{-1}\boldsymbol{k}}$, the Berry connection transforms as

$$\mathcal{A}^{\alpha}_{\boldsymbol{k}mn} = i\sum_{p}[(\mathcal{M}U)^{\dagger}_{\mathcal{M}^{-1}\boldsymbol{k}}]_{mp}\frac{\partial(\mathcal{M}U_{\mathcal{M}^{-1}\boldsymbol{k}})_{pn}}{\partial k_{\alpha}} = i\sum_{p}\frac{(\partial M^{-1}\boldsymbol{k})^{\beta}}{\partial \boldsymbol{k}^{\alpha}}[(\mathcal{M}U)^{\dagger}_{\mathcal{M}^{-1}\boldsymbol{k}}]_{mp}\frac{\partial(\mathcal{M}U_{\mathcal{M}^{-1}\boldsymbol{k}})_{pn}}{\partial(\mathcal{M}^{-1}\boldsymbol{k})_{\beta}} = \mathcal{M}_{\alpha\beta}\mathcal{A}^{\beta}_{\mathcal{M}^{-1}\boldsymbol{k}mn}. \tag{E81}$$

The derivative operation transforms as

$$\frac{\partial g_{\boldsymbol{k}m}}{\partial \boldsymbol{k}_{\alpha}} = \frac{(\partial M^{-1}\boldsymbol{k})_{\beta}}{\partial \boldsymbol{k}_{\alpha}}\frac{\partial g_{\mathcal{M}^{-1}\boldsymbol{k}m}}{\partial \boldsymbol{k}_{\alpha}} = \mathcal{M}_{\alpha\beta}\frac{\partial g_{\mathcal{M}^{-1}\boldsymbol{k}m}}{\partial \boldsymbol{k}_{\alpha}}. \tag{E82}$$

[1] I. Žutić, J. Fabian, and S. Das Sarma, Spintronics: Fundamentals and applications, Rev. Mod. Phys. **76**, 323 (2004).

[2] S. D. Bader and S. Parkin, Spintronics, Annu. Rev. Condens. Matter Phys. **1**, 71 (2010).

[3] A. V. Chumak, V. I. Vasyuchka, A. A. Serga, and B. Hillebrands, Magnon spintronics, Nat. Phys. **11**, 453 (2015).

[4] V. Baltz, A. Manchon, M. Tsoi, T. Moriyama, T. Ono, and Y. Tserkovnyak, Antiferromagnetic spintronics, Rev. Mod. Phys. **90**, 015005 (2018).

[5] S. Seki, T. Ideue, M. Kubota, Y. Kozuka, R. Takagi, M. Nakamura, Y. Kaneko, M. Kawasaki, and Y. Tokura, Thermal generation of spin current in an antiferromagnet, Phys. Rev. Lett. **115**, 266601 (2015).

[6] S. M. Wu, W. Zhang, A. KC, P. Borisov, J. E. Pearson, J. S. Jiang, D. Lederman, A. Hoffmann, and A. Bhattacharya, Antiferromagnetic spin seebeck effect, Phys. Rev. Lett. **116**, 097204 (2016).

[7] H. Katsura, N. Nagaosa, and P. A. Lee, Theory of the thermal Hall effect in quantum magnets, Phys. Rev. Lett. **104**, 066403 (2010).

[8] Y. Onose, T. Ideue, H. Katsura, Y. Shiomi, N. Nagaosa, and Y. Tokura, Observation of the magnon Hall effect, Science **329**, 297 (2010).

[9] R. Matsumoto and S. Murakami, Theoretical prediction of a rotating magnon wave packet in ferromagnets, Phys. Rev. Lett. **106**, 197202 (2011).

[10] R. Cheng, S. Okamoto, and D. Xiao, Spin nernst effect of magnons in collinear antiferromagnets, Phys. Rev. Lett. **117**, 217202 (2016).

[11] V. A. Zyuzin and A. A. Kovalev, Magnon spin nernst effect in antiferromagnets, Phys. Rev. Lett. **117**, 217203 (2016).

[12] B. Li, S. Sandhoefner, and A. A. Kovalev, Intrinsic spin nernst effect of magnons in a noncollinear antiferromagnet, Phys. Rev. Res. **2**, 013079 (2020).

[13] I. Proskurin, A. S. Ovchinnikov, J. I. Kishine, and R. L. Stamps, Excitation of magnon spin photocurrents in antiferromagnetic insulators, Phys. Rev. B **98**, 134422 (2018).

[14] H. Ishizuka and M. Sato, Theory for shift current of bosons: Photogalvanic spin current in ferrimagnetic and antiferromagnetic insulators, Phys. Rev. B **100**, 224411 (2019).

[15] H. Ishizuka and M. Sato, Large photogalvanic spin current by magnetic resonance in bilayer cr trihalides, Phys. Rev. Lett. **129**, 107201 (2022).

[16] E. V. n. Boström, T. S. Parvini, J. W. McIver, A. Rubio, S. V. Kusminskiy, and M. A. Sentef, All-optical generation of antiferromagnetic magnon currents via the magnon circular photogalvanic effect, Phys. Rev. B **104**, L100404 (2021).

[17] Y. Takahashi, R. Shimano, Y. Kaneko, H. Murakawa, and Y. Tokura, Magnetoelectric resonance with electromagnons in a perovskite helimagnet, Nat. Phys. **8**, 121 (2012).

[18] I. Kézsmárki, N. Kida, H. Murakawa, S. Bordács, Y. Onose, and Y. Tokura, Enhanced directional dichroism of terahertz light in resonance with magnetic excitations of the multiferroic $ba_2coge_2o_7$ oxide compound, Phys. Rev. Lett. **106**, 057403 (2011).

[19] S. Bordács, I. Kézsmárki, D. Szaller, L. Demkó, N. Kida, H. Murakawa, Y. Onose, R. Shimano, T. Room, U. Nagel *et al.*, Chirality of matter shows up via spin excitations, Nat. Phys. **8**, 734 (2012).

[20] K. Fujiwara, S. Kitamura, and T. Morimoto, Nonlinear spin current of photoexcited magnons in collinear antiferromagnets, Phys. Rev. B **107**, 064403 (2023).

[21] P. A. McClarty, Topological magnons: A review, Annu. Rev. Condens. Matter Phys. **13**, 171 (2022).

[22] Y. Aharonov and A. Casher, Topological quantum effects for neutral particles, Phys. Rev. Lett. **53**, 319 (1984).

[23] M. Ericsson and E. Sjöqvist, Towards a quantum Hall effect for atoms using electric fields, Phys. Rev. A **65**, 013607 (2001).

[24] T. Liu and G. Vignale, Electric control of spin currents and spin-wave logic, Phys. Rev. Lett. **106**, 247203 (2011).

[25] S. Toth and B. Lake, Linear spin wave theory for single-q incommensurate magnetic structures, J. Phys.: Condens. Matter **27**, 166002 (2015).

[26] R. Shindou, R. Matsumoto, S. Murakami, and J. I. Ohe, Topological chiral magnonic edge mode in a magnonic crystal, Phys. Rev. B **87**, 174427 (2013).

[27] F. Meier and D. Loss, Magnetization transport and quantized spin conductance, Phys. Rev. Lett. **90**, 167204 (2003).

[28] K. Nakata, J. Klinovaja, and D. Loss, Magnonic quantum Hall effect and wiedemann-franz law, Phys. Rev. B **95**, 125429 (2017).

[29] S. A. Owerre, Floquet topological magnons, J. Phys. Commun. **1**, 021002 (2017).

[30] K. Nakata, S. K. Kim, and S. Takayoshi, Laser control of magnonic topological phases in antiferromagnets, Phys. Rev. B **100**, 014421 (2019).

[31] J. L. Cheng, N. Vermeulen, and J. E. Sipe, Third-order nonlinearity of graphene: Effects of phenomenological relaxation and finite temperature, Phys. Rev. B **91**, 235320 (2015).

[32] G. B. Ventura, D. J. Passos, J. M. B. Lopes dos Santos, J. M. Viana Parente Lopes, and N. M. R. Peres, Gauge covariances and nonlinear optical responses, Phys. Rev. B **96**, 035431 (2017).

[33] S. D. Ganichev, E. L. Ivchenko, S. N. Danilov, J. Eroms, W. Wegscheider, D. Weiss, and W. Prettl, Conversion of spin into directed electric current in quantum wells, Phys. Rev. Lett. **86**, 4358 (2001).

[34] K. Hamamoto, M. Ezawa, K. W. Kim, T. Morimoto, and N. Nagaosa, Nonlinear spin current generation in noncentrosymmetric spin-orbit coupled systems, Phys. Rev. B **95**, 224430 (2017).

[35] H. Kondo and Y. Akagi, Nonlinear magnon spin nernst effect in antiferromagnets and strain-tunable pure spin current, Phys. Rev. Res. **4**, 013186 (2022).

[36] A. P. Kirk and D. W. Cardwell, Reconsidering the shockley–queisser limit of a ferroelectric insulator device, Nat. Photon. **11**, 329 (2017).

[37] H. Watanabe and Y. Yanase, Chiral photocurrent in parity-violating magnet and enhanced response in topological antiferromagnet, Phys. Rev. X **11**, 011001 (2021).

[38] Z. Dai and A. M. Rappe, Recent progress in the theory of bulk photovoltaic effect, Chem. Phys. Rev. **4**, 011303 (2023).

[39] A. Pusch, U. Römer, D. Culcer, and N. J. Ekins-Daukes, Energy conversion efficiency of the bulk photovoltaic effect, PRX Energy **2**, 013006 (2023).

[40] T. Morimoto and N. Nagaosa, Topological nature of nonlinear optical effects in solids, Sci. Adv. **2**, e1501524 (2016).

[41] B. M. Fregoso, T. Morimoto, and J. E. Moore, Quantitative relationship between polarization differences and the zone-averaged shift photocurrent, Phys. Rev. B **96**, 075421 (2017).

[42] H. Chen, Q. Niu, and A. H. MacDonald, Anomalous Hall effect arising from noncollinear antiferromagnetism, Phys. Rev. Lett. **112**, 017205 (2014).

[43] M.-T. Suzuki, T. Koretsune, M. Ochi, and R. Arita, Cluster multipole theory for anomalous Hall effect in antiferromagnets, Phys. Rev. B **95**, 094406 (2017).

[44] K. Essafi, L. Jaubert, and M. Udagawa, Flat bands and dirac cones in breathing lattices, J. Phys.: Condens. Matter **29**, 315802 (2017).

[45] R. Schaffer, Y. Huh, K. Hwang, and Y. B. Kim, Quantum spin liquid in a breathing kagome lattice, Phys. Rev. B **95**, 054410 (2017).

[46] M. Ezawa, Higher-order topological insulators and semimetals on the breathing kagome and pyrochlore lattices, Phys. Rev. Lett. **120**, 026801 (2018).

[47] A. Bolens and N. Nagaosa, Topological states on the breathing kagome lattice, Phys. Rev. B **99**, 165141 (2019).

[48] F. Zhuo, H. Li, and A. Manchon, Topological phase transition and thermal Hall effect in kagome ferromagnets, Phys. Rev. B **104**, 144422 (2021).

[49] S. Hayami and T. Matsumoto, Essential model parameters for nonreciprocal magnons in multisublattice systems, Phys. Rev. B **105**, 014404 (2022).

[50] Y. Ferreiros and M. A. H. Vozmediano, Elastic gauge fields and Hall viscosity of dirac magnons, Phys. Rev. B **97**, 054404 (2018).

[51] S. Owerre, Strain-induced topological magnon phase transitions: Applications to kagome-lattice ferromagnets, J. Phys.: Condens. Matter **30**, 245803 (2018).

[52] A. Mook, J. Henk, and I. Mertig, Magnon Hall effect and topology in kagome lattices: A theoretical investigation, Phys. Rev. B **89**, 134409 (2014).

[53] L. Cornelissen, J. Liu, R. Duine, J. B. Youssef, and B. Van Wees, Long-distance transport of magnon spin information in a magnetic insulator at room temperature, Nat. Phys. **11**, 1022 (2015).

[54] J. G. Rau, L. S. Wu, A. F. May, L. Poudel, B. Winn, V. O. Garlea, A. Huq, P. Whitfield, A. E. Taylor, M. D. Lumsden, M. J. P. Gingras, and A. D. Christianson, Anisotropic exchange within decoupled tetrahedra in the quantum breathing pyrochlore $Ba_3Yb_2Zn_5O_{11}$, Phys. Rev. Lett. **116**, 257204 (2016).

[55] A. Akbari-Sharbaf, R. Sinclair, A. Verrier, D. Ziat, H. D. Zhou, X. F. Sun, and J. A. Quilliam, Tunable quantum spin liquidity in the 1/6th-filled breathing kagome lattice, Phys. Rev. Lett. **120**, 227201 (2018).

[56] M. Hirschberger, T. Nakajima, S. Gao, L. Peng, A. Kikkawa, T. Kurumaji, M. Kriener, Y. Yamasaki, H. Sagayama, H. Nakao *et al.*, Skyrmion phase and competing magnetic orders on a breathing kagomé lattice, Nat. Commun. **10**, 5831 (2019).

[57] S. V. Gallego, J. M. Perez-Mato, L. Elcoro, E. S. Tasci, R. M. Hanson, K. Momma, M. I. Aroyo, and G. Madariaga, Magndata: towards a database of magnetic structures. i. the commensurate case, J. Appl. Crystallogr. **49**, 1750 (2016).

[58] A. Kamra and W. Belzig, Super-poissonian shot noise of squeezed-magnon mediated spin transport, Phys. Rev. Lett. **116**, 146601 (2016).

[59] W. Brenig and A. L. Chernyshev, Highly dispersive scattering from defects in noncollinear magnets, Phys. Rev. Lett. **110**, 157203 (2013).

[60] C. Kittel and C.-y. Fong, *Quantum Theory of Solids* (Wiley, New York, 1963), Vol. 5.

[61] W. Nolting and A. Ramakanth, *Quantum Theory of Magnetism* (Springer Science & Business Media, New York, 2009).

[62] S. Petit, Numerical simulations and magnetism, École Thém. Soc. Française Neutroniq. **12**, 105 (2011).

[63] K. Nakata, S. K. Kim, J. Klinovaja, and D. Loss, Magnonic topological insulators in antiferromagnets, Phys. Rev. B **96**, 224414 (2017).

[64] M.-w. Xiao, Theory of transformation for the diagonalization of quadratic hamiltonians, arXiv:0908.0787.

[65] J. Ahn, G.-Y. Guo, and N. Nagaosa, Low-frequency divergence and quantum geometry of the bulk photovoltaic effect in topological semimetals, Phys. Rev. X **10**, 041041 (2020).

[66] S. Tsirkin and I. Souza, On the separation of Hall and ohmic nonlinear responses, SciPost Phys. Core **5**, 039 (2022).

[67] J. E. Sipe and A. I. Shkrebtii, Second-order optical response in semiconductors, Phys. Rev. B **61**, 5337 (2000).